Structure of the Havallah sequence, Golconda allochthon, Nevada: Evidence for prolonged evolution in an accretionary prism

HANNES K. BRUECKNER *Department of Earth and Environmental Sciences, Queens College of CUNY, Flushing, New York 11367* and *Lamont-Doherty Geological Observatory, Columbia University, Palisades, New York 10964*
WALTER S. SNYDER *Department of Geology and Geophysics, Boise State University, Boise, Idaho 83725*

ABSTRACT

The Golconda allochthon of northern and central Nevada contains the Havallah sequence and correlative units of latest Devonian to early Late Permian age. The Havallah sequence is dominated by radiolarian ribbon chert and argillite associated with variable, but generally subordinate, siliciclastic, calcarenitic, and volcaniclastic turbidites and slump deposits. Cherts of all ages (except Pennsylvanian?) locally rest depositionally on tholeiitic basalts. Some were altered and mineralized by ridge-type hydrothermal systems, suggesting deposition in an ocean basin containing active spreading center(s) for much of the upper Paleozoic.

The Havallah sequence was thrust eastward along the basal Golconda thrust onto coeval sediments of the western North American shelf during the latest Paleozoic–earliest Mesozoic Sonoma orogeny. Detailed studies of the Havallah sequence in the Sonoma and Tobin Ranges and in Battle Mountain indicate the presence of complex diagenetic and structural fabrics that developed prior to the obduction of the allochthon. A large number of thrusts, composite thrusts, and shear zones slice the Havallah into numerous tectonic packets of contrasting lithology and/or internal structural style. Internal structures in chert packets include bedding-parallel and bedding-normal solution cleavage, solution boudins, three or more sets of east-verging folds of variable geometry, and features associated with high pore-fluid pressures such as crack-seal fractures, dilation breccias, clastic dikes and sills, and clastic intrusions along thrust surfaces. The fabrics suggest a general progressive evolution from deformation characterized by bedding-normal compression and slight east-west extension (D_1) to deformation dominated by bedding-parallel, east-directed shear (D_2). Local chert packets may have suffered alternating episodes of high and low pore-fluid pressure. The degree of development and the styles and orientations of various structural elements vary, sometimes radically, from packet to packet.

The pre-Golconda thrust fabrics can be modeled as the result of imbrication and deformation of successive batches of ocean-floor sediments into the toe of an accretionary prism in front of an east-facing arc. Relatively undeformed Permian calcarenite units, interpreted as being trench-slope deposits, suggest that this prism was well developed by Permian time. Coarse slump deposits containing chert clasts with pre-depositional structural fabrics suggest a prism that was active long enough to recycle previously tectonized cherts. If we are correct, the classical Sonoma orogeny (D_3) marked the culmination of a protracted structural evolution that may have spanned much of the upper Paleozoic.

INTRODUCTION

The upper Paleozoic Havallah sequence is a chert-turbidite-greenstone complex that is exposed in several ranges in northern and central Nevada (Fig. 1). It is an oceanic suite containing (1) tholeiitic pillow lavas; (2) massive sulfide and siliceous Fe and Mn mineral deposits; (3) pelagic and hemipelagic sediments, including ribbon radiolarian chert and argillite; (4) siliciclastic and calcarenitic turbidite deposits that include slump breccias; and (5) local volcaniclastic turbidites and breccias. Its age, based on radiolaria, conodonts, and fusulinids, ranges from Late Devonian–Early Mississippian to early Late Permian (Roberts, 1964; Erickson and Marsh, 1974; Silberling, 1973, 1975; Stewart and others, 1977 and unpub. data; Miller and others, 1982, 1984; Laule and others, 1981 and unpub. data). The Havallah sequence is allochthonous and was transported eastward along the Golconda thrust over coeval autochthonous shallow-marine and nonmarine assemblages and older deformed rocks of the Roberts Mountain allochthon during the Late Permian and/or Early Triassic Sonoma orogeny (Silberling and Roberts, 1962).

The depositional setting of the Havallah sequence and the mechanisms of its emplacement are debated (see Snyder and Brueckner, 1983, and Miller and others, 1984, for most recent reviews). The presence of upper Paleozoic tholeiitic pillow lavas and associated ridge-type hydrothermal deposits (Snyder, 1977, 1978; Rye and others, 1984) indicates that the basement to Havallah sediments was oceanic crust. Several investigators (Burchfiel and Davis, 1975; Miller and others, 1982, 1984; Whiteford and others, 1983) advocate deposition of the Havallah sequence in a back-arc basin behind a nearby west-facing arc with subsequent back-arc thrusting when the basin closed. Others (Speed, 1977, 1979; Dickinson, 1977; Schweickert and Snyder, 1981; Snyder and Brueckner, 1983) favor deposition in a relatively large ocean basin with development of an accretionary wedge in front of an east-facing island arc. The island arc–accretionary prism complex may have traveled a long way before colliding with North America and thrusting the accretionary wedge over the continental margin.

This paper concentrates on describing the structural fabric of part of the Havallah sequence in the Galena Range (Battle Mountain), Edna Mountain, and the Sonoma, Tobin, and Toquima Ranges, with particular emphasis on small-scale structures in cherts. Closely spaced thrusts within the Havallah sequence have resulted in the juxtaposition of innumerable fault-bounded structural units that we call tectonic packets. Each packet has an internal structural fabric which varies, sometimes markedly, from packet to packet. Measurements collected over large-scale domains (hillsides, entire ranges, and so forth) and presented on summary diagrams tend to produce a pseudo-uniform fabric that obscures some important structural variations between packets. This paper presents some summary and representative, packet-by-packet

Geological Society of America Bulletin, v. 96, p. 1113–1130, 14 figs., 1 table, September 1985.

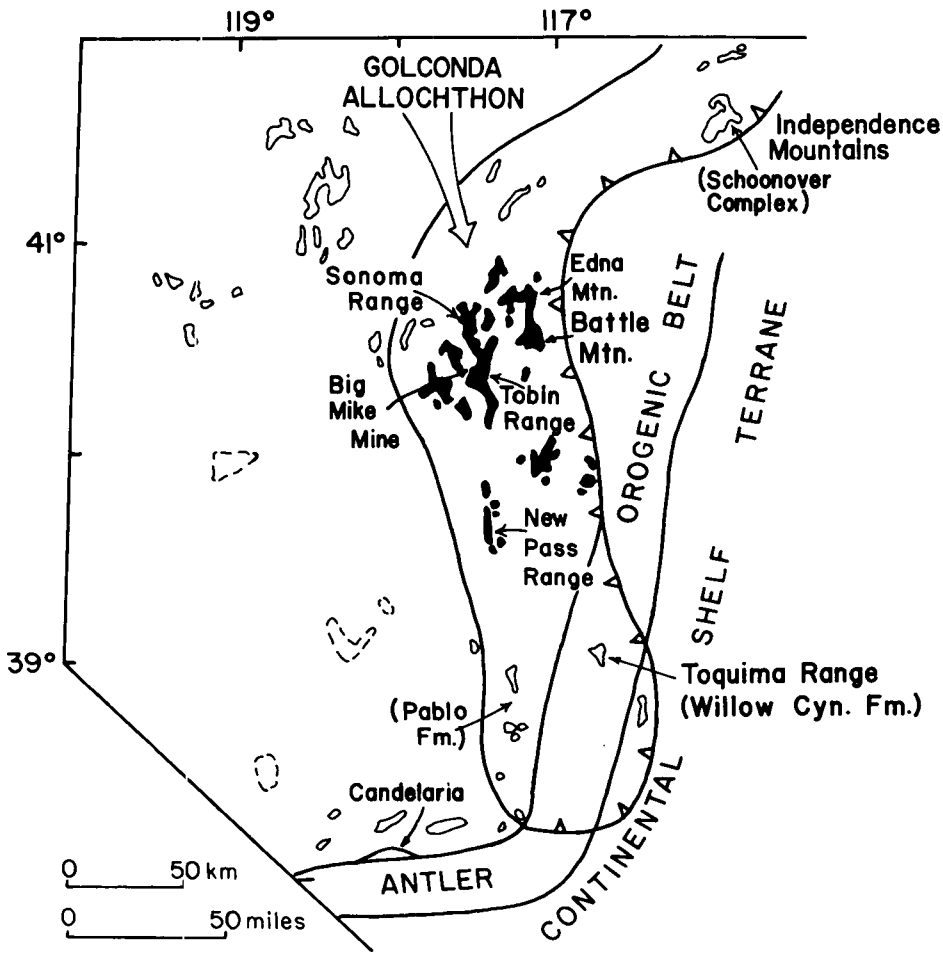

Figure 1. Upper Paleozoic paleogeographic map of Nevada showing the relationships between the Golconda allochthon, the Antler orogenic belt and continental shelf sediments, modified from Speed (1977) and Stewart and others (1977). Exposures of the Havallah sequence are shown as solid black. The names of correlative units are enclosed in parentheses. The position of the Golconda thrust along the eastern margin of the allochthon is schematic.

measurements to illustrate this conclusion. Results of the far more numerous measurements not presented here are available on request from both authors.

Our study of fabrics in various tectonic packets suggests that the strain histories of Havallah siliceous sediments were complex and polyphase, implying a protracted strain history for the Havallah sequence as a whole. Furthermore, the amount of telescoping recorded by the large number of these fault-bounded packets is probably much greater than has been generally recognized. We suggest that an extended structural evolution and a large degree of structural shortening is in reasonable accord with the far-traveled accretionary prism interpretation. Accordingly, we model the tectonic history of the Havallah as the continuous shuffling of a thin veneer of oceanic sediments into an accretionary wedge that persisted for a significant span of geologic time before it was emplaced along the Golconda thrust onto North America.

GENERAL STRUCTURE

The structure of the Havallah sequence is dominated by thrusts. The best documented is the basal Golconda thrust which, though rarely exposed, is recognized by the juxtaposition of the Havallah sequence with coeval shelf sediments. Major thrusts within the sequence have been recognized by the juxtaposition of units of different age and/or lithology in Hoffman Canyon of the Tobin Range (Ferguson and others, 1951a, 1951b, 1952; Stewart and others, 1977 and unpub. data), the New Pass Range (Macmillan, 1972), Willow Creek in Battle Mountain (Roberts, 1964; Miller and others, 1982; this work), the Independence Range (Miller and others, 1981, 1984), the Toquima Range (Laule and others, 1981 and unpub. data), as well as in other parts of the Sonoma and Tobin Ranges (this work). Figure 2 is a preliminary compilation of the distribution of the major lithotectonic units bounded by the major thrusts in Battle Mountain and by the Tobin and Sonoma Ranges (see Fig. 2 for references).

The lithotectonic units are, in turn, cut by numerous internal bedding-parallel thrust faults which divide chert, turbidite, and argillite into *tectonic packets* which may be a few centimetres to tens of metres thick and several metres to hundreds of metres long (Fig. 3). The chert packets are characterized by different degrees and styles of deformation from packet to packet. Some packets (for example, unit J in Fig. 3) contain undeformed beds of constant thickness along strike. Beds in other packets are characterized by strong boudin-like fabrics which range from pseudo pinch-and-swell structures to blocks with more angular profiles separated by high-angle fractures (unit B). Still other packets expose from one (unit K) to three generations of roughly coaxial folds (unit H).

Virtually undeformed cherts can be found in direct contact with packets containing highly deformed strata (units J and K, respectively, Fig. 3). Similar generalizations can be made for the Havallah sequence in the Tobin, Sonoma, and Toquima Ranges and Edna and Fish Creek Mountains. Most chert packets in the Havallah sequence are bounded by thrust faults which ultimately cut off individual units along strike; thus, there is not necessarily an orderly stratigraphic succession perpendicular to strike and limited structural continuity parallel to strike. The rarely exposed contacts between different rock types are generally, although not always, tectonic.

The displacements along these fault zones are unknown. Faults that juxtapose faunal assemblages of different ages are assumed to have undergone significant displacements and are mapped as major thrusts (Fig. 2) which define the major lithotectonic units. Faults that juxtapose different lithologies (that is, chert-argillite, chert-turbidite, and so forth) or chert packets of distinctively different structural style are assumed to have suffered appreciable movement, but the amount of displacement is unknown. By dividing most, if not all, of the lithotectonic units into numerous planar, subparallel tectonic packets, these internal thrusts give the Havallah sequence a deceptively simple homoclinal appearance in most areas (see Fig. 3) and obscures the complicated internal features contained in some of the chert packets. The following sections describe these features and provide some

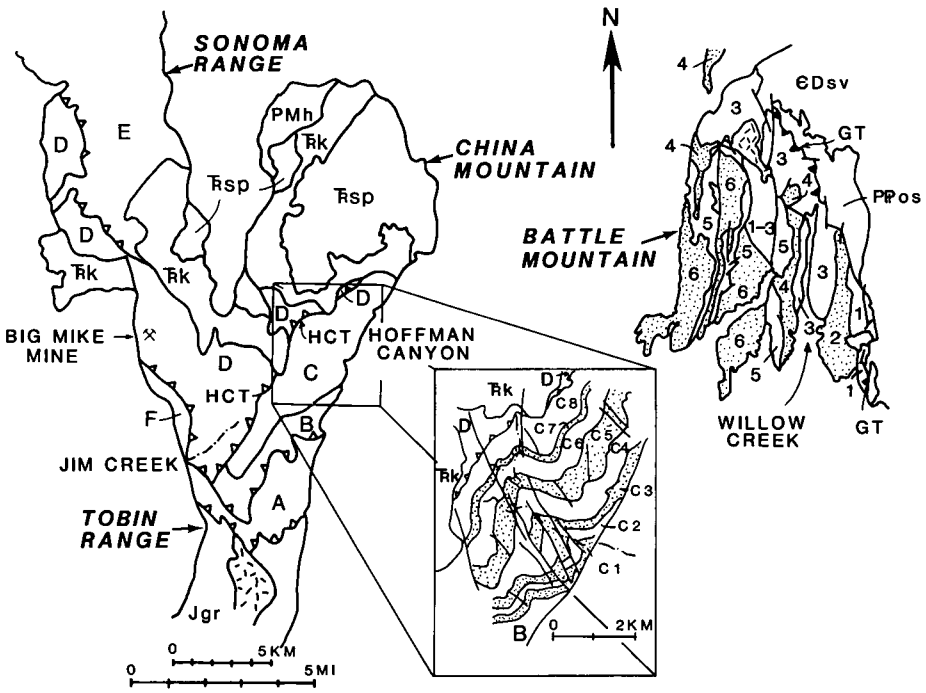

Figure 2. Generalized tectonic map of the Havallah sequence in the Sonoma and Tobin Ranges and the Antler Peak area (Battle Mountain). Units A through F in the Sonoma and Tobin Ranges are major thrust-bounded lithotectonic units defined by age differences or major changes in lithology (Muller and others, 1951; Ferguson and others, 1951a, 1951b, 1952; Stewart and others, 1977; Snyder, unpub. data). Inset is a more detailed map of Hoffman Canyon, Tobin Range, showing the division of lithotectonic unit C into tectonic packets C1 through C8 (Stewart and others, 1977 and unpub. data). The thrust between lithotectonic units C and D is the Hoffman Canyon thrust (HCT) (Ferguson and others, 1952). Units 1 through 8 in Battle Mountain are lithotectonic units mapped largely on lithology (Roberts, 1951, 1964) and, near the Golconda thrust radiolarian ages (Miller and others, 1982). Packets from unit 3 near the Golconda thrust (at arrow labeled GT) are shown in the cross section in Figure 3. ϵDsv, lower Paleozoic units of the Roberts Mountain allochthon; IPos, Pennsylvanian-Permian overlap sequence; IPMh, Pennsylvanian-Mississippian Havallah sequence; ŦrK, Lower Triassic Koipato Group; Ŧsp, Triassic Star Peak group; Jgr, Jurassic granite.

representative data. The distinction between sedimentary (diagenetic) and tectonic features is not always clear; furthermore, ordering features from different packets into a chronological sequence is somewhat subjective. For these reasons, a separate section is devoted to these problems.

FRACTURES

Bedding-Normal Fractures

Virtually all chert layers contain numerous fractures that are approximately perpendicular to bedding but otherwise display no preferred orientations. Each fracture affects only a single bed or a few beds. Crosscutting relationships suggest several generations of fractures. Some fractures underwent dip-slip motion; others apparently simply dilated and are filled with chalcedony, macrocrystalline quartz, or both. A few fractures contain several generations of vein material.

Step Planes

These fractures are distinguished from those discussed above by having a strong preferred orientation (Fig. 4A). Most have suffered dip-slip motion and offset the previously formed bedding-normal fractures. The fractures are not simple high-angle faults because individual fractures affect only a single bed or a few beds, and the amount of apparent offset changes as the fractures are traced downdip (Fig. 4B). The intersection of these fractures with offset bedding surfaces creates little steps (Fig. 4A); hence, we tentatively call these fractures "step planes" and the intersection of the step planes with bedding, "step lines." Step planes commonly segment the chert layers into prisms with rhomboid profiles.

PRESSURE-SOLUTION-RELATED FEATURES

Bedding-Parallel Microstylolites

Clays and unidentified opaque material in some siliceous layers are concentrated as films and trains into micron-thick laminae (Fig. 5). The laminae form an anastomosing, subparallel network that parallels chert layering, is locally stylolitic, and abuts against partially dissolved radiolaria. We interpret these structures as being insoluble residues which were left after the dissolution and removal of silica, similar in origin to the microstylolites described in limestone by Wanless (1979).

Microstylolites are lacking or widely spaced (several cm) in some chert layers and are more closely spaced (1 or 2 mm) in others. Quartz- and chalcedony-filled veins that formed before, or during, the creation of the microstylolites and were oriented at high angles to bedding are straight and undeformed in microstylolite-poor layers but crumpled where they occur in microstylolite-rich layers (Fig. 5). These veins are very strongly crumpled and locally brecciated in the thin (a few mm to 1 or 2 cm), argillite-rich partings that occur between the relatively clay-poor chert layers. The argillaceous partings thus are believed to be zones of merged or coalesced microstylolites that are rich in residual clay, similar to the microstylolite swarms and clay seams of Wanless (1979). If this interpretation is correct, it would suggest that the argillaceous partings are zones of considerable silica removal and may have suffered a large amount of thinning as a result of this process. This conclusion agrees with that of Jenkyns and Winterer (1982), who suggested that the chert-argillite couplet has been "diagenetically enhanced." It implies that the primary (that is, sedimentary) differences between the clay-rich and clay-poor layers of the ribbon chert couplet need not have been as great as they were after solution processes, and it obviates the need for radical changes in depositional processes to explain these differences. The strong planar fabric defined by bedding-parallel microstylolites is henceforth called a "microstylolite cleavage." Locally, folded microstylolites are crosscut by later, unfolded microstylolites (Turner, 1982).

Mound Structures

Irregular variations in thickness of some chert layers give them a knobby or moundlike ap-

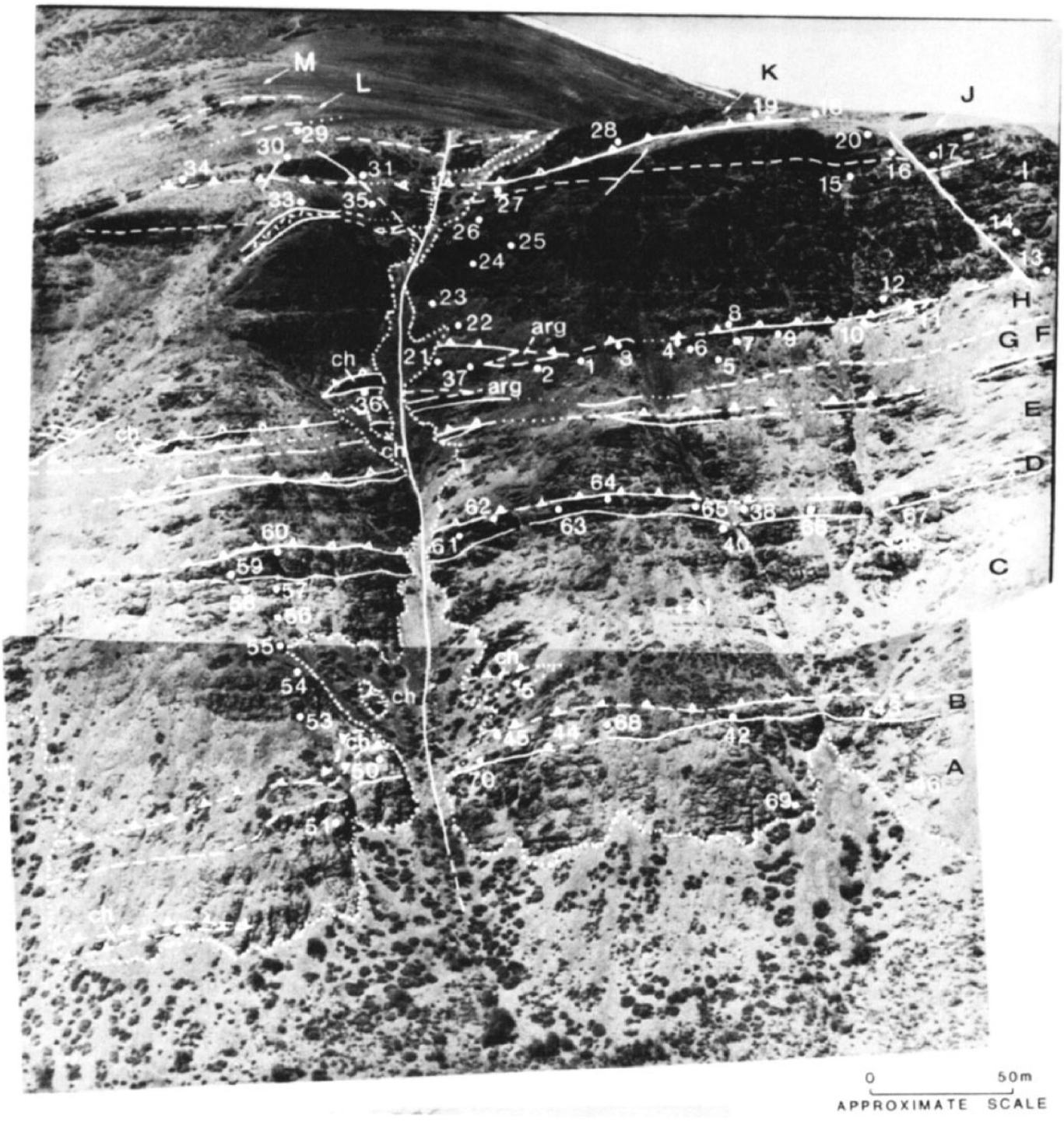

pearance. In plan view, the mounds have approximately circular outlines, with diameters ranging from 1 cm to tens of centimetres. They are invariably outlined by solution seams and many contain concentric rings composed of alternating quartz and chalcedony, similar to diagenetically produced growth rings in CT-chert nodules in the Monterey Formation (Taliaferro, 1934; Pisciotto, 1978; Snyder and others, 1983).

Solution-Modified Step Planes

Many step planes had their original, planar, clay-free configuration modified by pressure solution (Fig. 4B). They now have irregular profiles and are filled with clays and opaque material, suggesting that they become sites of silica dissolution, presumably because they acted as passages for the movement of fluids and as zones for stress concentration. Near the hinges of some folds, pressure solution during folding resulted in the reorientation of the step planes to near parallelism with the axial surface of the fold. Near other hinges, the step planes were simply fanned about the fold hinge. The degree of reorientation by pressure solution varies from fold to fold and from layer to layer and appears to reflect the solubility of the chert layer during

Figure 3. Tectonic packets in the basal portion of lithotectonic unit 3 (see Fig. 2) of the Golconda allochthon exposed on the west wall of Willow Creek Canyon, Battle Mountain. The Golconda thrust (covered) is just below the bottom of the figure. Units, A, C, E, G, I, and L are predominantly argillite. Units B, D, F, H, J, K, and M are dominated by bedded chert. Some of the contacts between the chert and argillite may be depositional (for example, J and I), others are clearly structural (for example, I and H, see truncated fold hinge at point 11; or unit J, which is unfolded, and unit K, which is intensely folded). Numbers mark stations. Photo taken from helicopter; view is to the west.

folding (Brueckner and others, unpub. data). Many of the fanned and/or axial-surface fracture patterns observed in folded chert may have originated as step planes prior to folding.

Solution Boudins

The step-plane fabric is believed to have influenced the development of a "boudin" fabric (previously called "lenticle fabric"; Snyder and Brueckner, 1983) that we suggest formed largely through the differential removal of silica from chert layers. Many chert packets are characterized by layers that are alternately thick and thin along strike (Fig. 6). The upper and lower boundaries of the thick portions are weakly to strongly convex outward, producing elliptical or lensoid profiles. These features are similar to Monroe structures, except that they are weakly to strongly elongated parallel to bedding, defining a locally pronounced lineation. Clay-rich selvages ("argillite partings") separate the chert layers. The thick portion of one bed commonly fits into the thin portions of the overlying and underlying beds, producing a "nested" appearance (Fig. 6).

These features have been called "boudins" (Miller and others, 1982), and this term is appropriate if the original, purely descriptive, definition of boudins is retained; that is, they look like sausages lying side by side (see Ramsay, 1967). The boudins, however, are rarely pulled apart and hence bear a superficial resemblance to pinch-and-swell structures. This term is inappropriate, as there is little evidence that the chert layers were thinned or "pinched" by ductile extension parallel to bedding. Layers within the thin portions of a chert bed are not thinner or more closely spaced than they are within the thick portions.

We feel that these structures formed largely by a silica dissolution process (Brueckner and others, unpub. data) rather than by ductile necking. Layers within the thick portions of the chert bed are terminated along their convex-outward boundaries by the argillite partings that we judge to be solution seams. The thin portions of the beds are therefore believed to be zones of considerable silica removal. This relationship is illustrated on a microscopic scale (Fig. 5) where chert layers of irregular thickness and lensoid chert residues are entirely surrounded by microstylolites. We suggest that the thick portions of chert beds be called "solution boudins"; the thin portions, "solution necks"; and the resultant linear fabric, "solution-boudin lines."

Step lines and solution-boudin lines are almost invariably parallel in any chert packet. The steps created by the intersection of step planes and bedding are sharp and well defined in chert layers that lack solution boudins (Fig. 4A) and become progressively rounded and less well defined as the solution-boudin fabric becomes better developed. Steps are usually not obvious in layers with strongly developed solution-boudin fabrics (Fig. 6); however, many solution necks contain fractures or vein-filled fractures, some of which have undergone dip-slip motion. We believe that some of these fractures are step planes, strongly modified by silica dissolution (Fig. 4B). We suggest that the formation of step planes created passages for the movement of aqueous solutions and caused silica dissolution to be concentrated along the strike of the step planes, resulting in the formation of solution necks and the strong preferred orientation of the solution-boudin lines. Our hypothesis therefore requires minor brittle extension to form the step planes, and bedding-parallel pressure solution to form the solution-boudin fabric.

Figure 7 plots the orientations of undifferentiated step lines and solution-boudin lines on the lower hemispheres of equal-area nets. Figure 7A is a summary diagram of all measured lines from the Tobin Range. Although most plunge toward the north at shallow to moderate angles, there is considerable scatter. The reasons for this scatter are shown in the succeeding diagrams (Figs. 7B, 7C, 7D) from three separate packets in unit D of the Tobin Range. Note that different packets display different patterns; some define strong point maximums (Figs. 7B and 7C), whereas a few others are variably distributed about a great circle which parallels bedding (Fig. 7D). Although the difference between adjacent packets is generally small (compare Figs. 7B and 7C), the cumulative effect over the entire range is significant.

The packet-to-packet variations may mean that rigid-body rotation during thrusting rotated these fabrics away from parallelism. The girdle versus point-maximum patterns of some adja-

Figure 4A. Step-plane fabric from unit H, Willow Creek, Battle Mountain (station 21, Fig. 3). Chert layers (horizontal) are cut by numerous step planes which create a staircase effect. The step planes have not been affected by later solution.

Figure 4B. Positive print of thin section (horizontal length = 2 cm) showing bedding and early-formed, bedding-parallel microstylolites offset by high-angle step planes. The step plane at right (A) is, in turn, cut by a later generation of bedding-parallel microstylolites and dies out upward and downward. A larger, braided step plane at left (B) suffered later pressure solution and acquired an irregular profile filled with insoluble material. Willow Canyon, Toquima Range.

cent packets also suggest, however, that the boudin–step-plane fabrics acquired different patterns and orientations at the time that they were imprinted on the siliceous sediments. The packet with the girdle distribution, for example, may not have had a strong step-plane fabric, and the varied orientations of the boudin lines were probably set by the random strikes of the early-formed, bedding-normal fractures.

High-Angle Solution Cleavage

There is at least one, and probably more, generation(s) of irregular to stylolitic, locally anastomosing laminae filled with clays and opaque material that are oriented at high angles to bedding (Fig. 5). The laminae appear to offset earlier features such as bedding-parallel microstylolites. We believe that these features constitute a high-angle solution cleavage similar to those described in cherts of the Crystalls Beach accretionary complex of New Zealand (Nelson, 1982). The spacing of solution cleavage varies from layer to layer; some layers contain abundant solution cleavage, whereas adjacent layers contain few or none.

The relation of these solution features to folds is still under investigation. Many fold hinges contain at least a few cleavage planes that crudely parallel the axial surface of the fold. Laminations that outline these hinges show abrupt angle changes across these cleavage surfaces, suggesting that pressure solution accompanied the development of these folds (Alvarez and others, 1976).

MESOSCOPIC FOLDS IN CHERT

Fold Geometries

Folds vary in style, orientation, and abundance from packet to packet. Representative fold profiles are illustrated in Figure 8. Truly isoclinal folds with long, planar limbs and very sharp hinges (Fig. 8A) are relatively rare, but tight folds with interlimb angles of 10°–30° are characteristic of many chert packets (Fig. 8B). Many of the folded layers are thicker in the hinges than in the limbs (Fig. 8B) and fall under classes 1C and 2, using the isogon classification method of Ramsay (1967). These layers apparently underwent intralayer ductile flow during deformation. Other chert packets are deformed by asymmetric chevron folds (Fig. 8C), typically with apical angles that range from 20° to 50° and amplitudes that range from 1 to 5 m. Chert layers are generally not thicker at the hinges than at the limbs, and most of these folds would be classified as 1B (Ramsay, 1967). Where they are developed, tight folds and chevron folds tend to harmonically deform the entire chert packet and are cut off by thrusts at the upper and lower packet boundaries.

Parallel or concentric folds (class 1B of Ramsay, 1967) are the most common folds in the Havallah sequence (Fig. 8D). They occur on all scales; amplitudes range from 0.3 to >30 m, although most range from 1 to 4 m. They exhibit typical disharmonic folding styles. Folds with curved limbs and broad open hinges change to tight folds and, in some cases, brecciated zones and thrust faults when traced along their axial surfaces (Fig. 8D). The degree of development of these folds varies from packet to packet; some packets contain only a few of these structures and are otherwise undeformed, whereas others are completely contorted internally.

Most of the smaller parallel folds (amplitudes between 0.3 and 4 m) occur within single thrust-bounded chert packets or deform a single thrust surface. Locally, these folds refold earlier tight to isoclinal folds (see also Miller and others, 1982, 1984; Macmillan, 1972 and unpub. data; Turner, 1982). Some very large folds deform several chert packets and the thrusts that bound these packets. For example, the fold which we call "Big Z" (Fig. 9) occurs just above the Hoffman Canyon thrust which separates unit D and unit C (Ferguson and others, 1952). It folds several thrust surfaces as well as one, and possibly two, sets of tight folds (Fig. 9), but it does not fold the Hoffman Canyon thrust. A similar, but

larger, fold occurs in Willow Canyon of the Toquima Range (Laule and others, unpub. data).

Box folds are scattered throughout the Havallah sequence, typically in chert packets that are otherwise not folded. The folds of opposite shear sense that define the corners of the boxes have small amplitudes (<0.2 m) and have curved, rather than kinked, profiles. The box folds usually merge with unfolded beds both upsection and downsection within <1 m.

Vergence

Virtually all folds are moderately to strongly asymmetric, and the great majority (~90%) are overturned toward the east. West-vergent folds normally are smaller (amplitudes of 0.1 to 1 m) and more open than are the east-verging folds. A few west-verging folds clearly deform both limbs of east-verging folds (Fig. 8C). Others occur on the short limbs of larger east-verging folds or occur together with east-verging folds to form box folds. Most commonly, however, the genetic relationships between east- and west-verging folds cannot be ascertained.

Relationships between Folds and Other Fabrics

All but two folds observed in the field deform the microstylolite cleavage. The exceptions are two isoclinal folds (Fig. 8A), where the microstylolite cleavage cuts across the fold hinge parallel to the axial surface of the fold. Some of the folds with either tight or chevron profiles display a second, generally weaker solution cleavage that is subparallel to the fold's axial surface. Chert layers in parallel folds are locally associated with spaced fractures which are either fanned or parallel to the axial surface. As noted above, some of these fractures are believed to be step planes that were rotated and subjected to variable pressure solution as the chert layers were folded.

Most solution-boudin lines and step lines parallel fold hinges (see below), but in all of the dozen or so observed examples where they are not parallel, the step and solution-boudin lines are folded about the hinges of the folds. Where they are parallel, there is a marked tendency for the fold hinge to occupy the thin solution necks between the solution boudins.

Chert packets that are harmonically deformed by folds with isoclinal, tight, and chevron profiles are almost invariably bounded by thrusts. Rootless hinges with these geometries are common in brecciated fault zones. Disharmonic parallel folds display a more complex relationship with thrusts. Some east-verging parallel folds are clearly offset by low-angle faults, but others fold

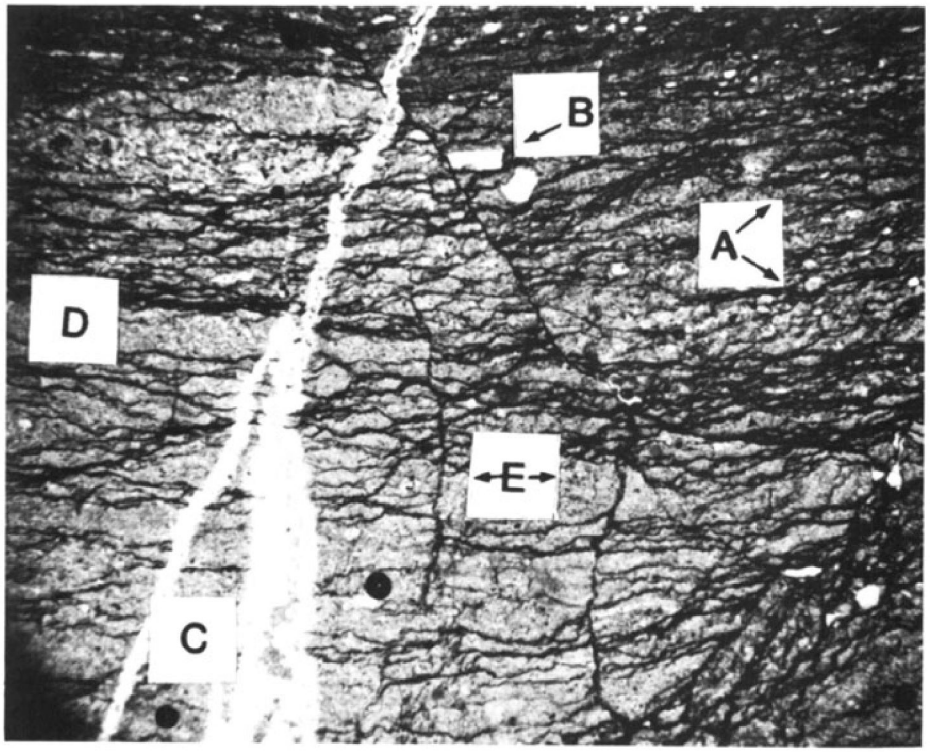

Figure 5. Positive photomicrograph (horizontal length = 0.5 cm) showing details of solution seam with bedding-parallel microstylolites (A, dark laminae), partially dissolved radiolarian test (B), and a crumpled antitaxial quartz vein (C). A "micro-solution boudin" fabric is defined by partially dissolved chert lenses in anastomosing microstylolites (D), which become more abundant upward. A few bedding-normal microstylolites cut the bedding-parallel set (E). Dark, circular spots are air bubbles.

Figure 6. Solution boudins in Mississippian cherts, Edna Mountain, with pseudo "pinch-and-swell" appearance. The thin, clay-rich "partings" (largely weathered-out in this example) are zones of coalesced microstylolites formed by the intense dissolution and removal of silica. Crests and troughs define a consistent north-plunging lineation. Note step planes in solution neck.

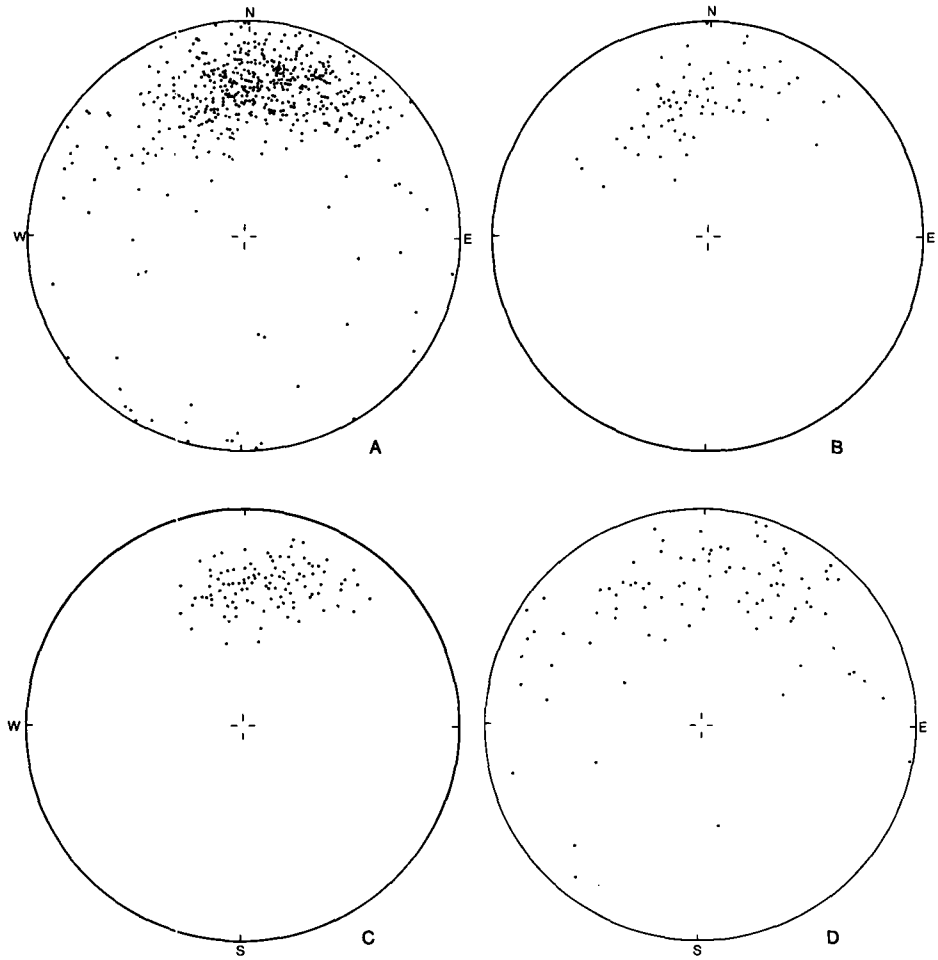

Figure 7. Equal-area plots of solution-boudin lines and step lines (dots) of the Havallah sequence, Tobin Range, Nevada. A. All measured lines from the entire Tobin Range. B. Lines from unit D-1 define a diffuse north to west-northwest–plunging maximum. C. Lines from unit D-2, immediately adjacent to unit D-1, with less diffuse maximum than from unit D-1 and north to north-northeast plunge. D. Lines from unit D-5 (Big Mike area) define a north-dipping girdle rather than the point maxima defined by units D-1 and D-2.

low-angle faults and associated brecciated zones. The large east-verging faults, such as Big Z, fold several chert packets and their bounding thrust surfaces but do not fold the large-scale thrusts that separate major lithotectonic units (Fig. 9). Most west-verging folds fold thrust surfaces or brecciated zones associated with thrust faults.

Fold Orientations

The orientation data presented in Figures 10 and 11 are meant to raise questions about the usefulness of regional summary diagrams when applied to a terrain dominated by numerous internal thrusts. The data are also meant to illustrate the difficulties encountered when trying to divide folds into generations on the basis of orientation alone. The hinges of all folds from the Tobin Range are plotted in Figure 10A. They define a girdle that dips at a shallow angle to the north-northwest with a well-defined, north-plunging maximum. This pattern is identical to that defined by step and boudin lines (Fig. 7A). The significance of these similar patterns is addressed in a later section. The poles to axial surfaces of these folds are plotted in Figure 10B and define a girdle with a north-plunging β axis that parallels the maximum defined by the hinges. The over-all fold fabric thus appears simple; however, there is considerable scatter to the data, and we suggest that this scatter hides information that is of considerable importance for interpreting the structural fabric of the Havallah sequence. For example, there is convincing field evidence that some chert packets have experienced more than one episode of folding (refolded folds, pre-, syn-, and post-thrust folds, and so forth). Folds that are either cut by thrust faults or are refolded are plotted separately (Fig. 10C) from folds that either postdate thrust faults or refold earlier folds (Fig. 10D) and are provisionally labeled "early" and "late" folds, respectively. Where these overprinting relationships are present, early folds tend to be class 1C or 2 folds with evidence of intralayer ductile deformation, whereas late folds tend to be disharmonic class 1B folds with little evidence of ductile flow within layers. Because most folds do not display clear overprinting relationships, we have used the somewhat subjective criteria of whether or not these folds show evidence of ductile flow to place them into the early or late set, respectively.

The hinges of early folds define a north-plunging maximum that is significantly displaced from the more northwesterly plunging maximum defined by late folds. There is considerable overlap, however, and it is this overlap that helps to produce the misleading maximum defined by plotting all fold hinges from the Tobin Range (Fig. 10A). The poles to axial surfaces of early folds define a girdle about a north-plunging β axis, whereas those of the "late" folds define a maximum, but, again, there is considerable overlap. Although the data verify field observations that the early folds were approximately coaxially refolded by late folds, individual folds cannot be assigned to either generation because of the overlap in their orientations. The relatively constant orientations of the axial surfaces of the late folds reflect the fact that early folds did not significantly perturb the relatively homoclinal configuration of the Havallah sequence because (1) many chert packets or parts of packets were not deformed by early folds; (2) early folds tend to be strongly overturned and tight, such that the fold limbs do not diverge radically from the orientation of regional bedding; and (3) many late folds deform thrust surfaces and thrust fabrics that generally parallel regional layering.

Hinges (X's) and poles to axial surfaces (circles containing X's) from late east-verging folds in the immediate vicinity of Big Z define slightly different patterns than do hinges (dots) and, particularly, poles to axial surfaces (empty circles) of late folds from the rest of the Tobin Range (Fig. 10D). Although we suspect that very large folds like Big Z are "very late" east-vergent structures, the small differences in orientation are not sufficient evidence to substantiate this suspicion.

West-vergent folds (Fig. 10E), some of which refold late east-verging folds, show less-orderly patterns than do the east-verging folds, as would be expected by printing new folds on surfaces

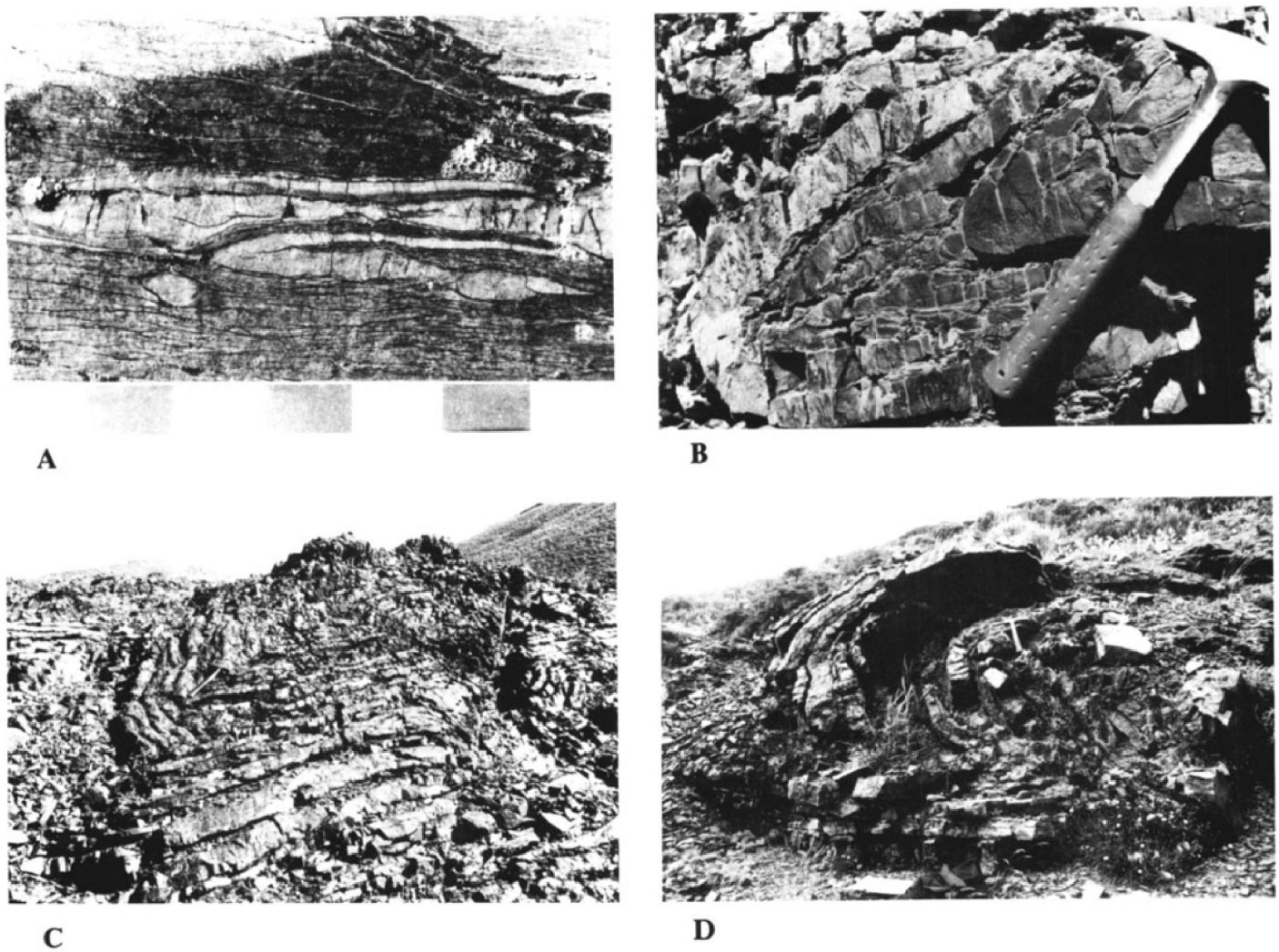

Figure 8. Fold fabric of the Havallah sequence, illustrating variable geometries of folds. A. Isoclinal fold in Mississipian cherts from Edna Mountain (scale in centimetres). Either the fold and microstylolite cleavage formed synchronously or the cleavage and solution boudins were overprinted on the fold. B. Tight fold from Permian cherts in Willow Creek, Battle Mountain. Note thickened hinges of some layers (for example, near hammer), suggesting ductile flow. Other layers brecciated, suggesting brittle behavior. C. Chevron fold in Pennsylvanian chert packet (northwest view) with overturned short limb and eastern vergence. Note small fold with opposite shear sense in upper right. Unit C-5, Hoffman Canyon, Tobin Range. D. Disharmonic, largely concentric, east-verging (southwest view) fold in unit B, Willow Creek, Battle Mountain. A low-angle thrust separates the upper hinge from the lower, tighter hinge.

that were complexly deformed, particularly by the disharmonic late east-verging folds. West-verging folds are generally small and sporadically developed and hence did not significantly reorient the fabric defined by east-verging folds; however, they contribute significantly to the scatter on the summary diagrams.

The deceptively simple-appearing summary fold fabrics obscure another very important aspect of the structural fabric of the Havallah sequence; namely, that the orientations (as well as geometries and abundances of different fold sets) vary from packet to packet, even within single lithotectonic units. Figures 11A, 11B, and 11C plot solution-boudin lines and fabrics of east-verging folds from three chert packets (units C-1, C-3, and C-5, respectively) within lithotectonic unit C in Hoffman Canyon, Tobin Range (Fig. 2). These chert packets are separated by relatively unfolded packets of calcareous sandstones. West-verging folds that clearly postdate east-verging folds are not plotted. Units C-1 and C-3 contain numerous internal thrusts and are actually composite packets; unit C-5 contains few or none. Unit C-1 (Fig. 11A) is dominated by open, asymmetric, post-thrust (late) folds. Their hinges (small dots) plunge northwest, for the most part, and do not parallel the largely north-plunging boudin lines (triangles). Axial surfaces (circled dots) dip northwest at moderate angles. Pre-thrust (early) folds (large dots) are rare.

Unit C-3 (Fig. 11B) contains abundant tight early folds (large dots) which are cut by internal thrusts. Rare post-thrust folds (small dots) and folds of uncertain relation to thrusts (X's) are also present. Hinges and solution-boudin lines (triangles) define parallel partial girdles which extend well to the northeast relative to the northwest-plunging hinges of folds in unit C-1. Axial surfaces of the pre-thrust, isoclinal folds (circles) consistently dip at shallow angles to the northwest.

Unit C-5 (Fig. 11C) is composed of trains of asymmetric chevron folds that are cut off at the

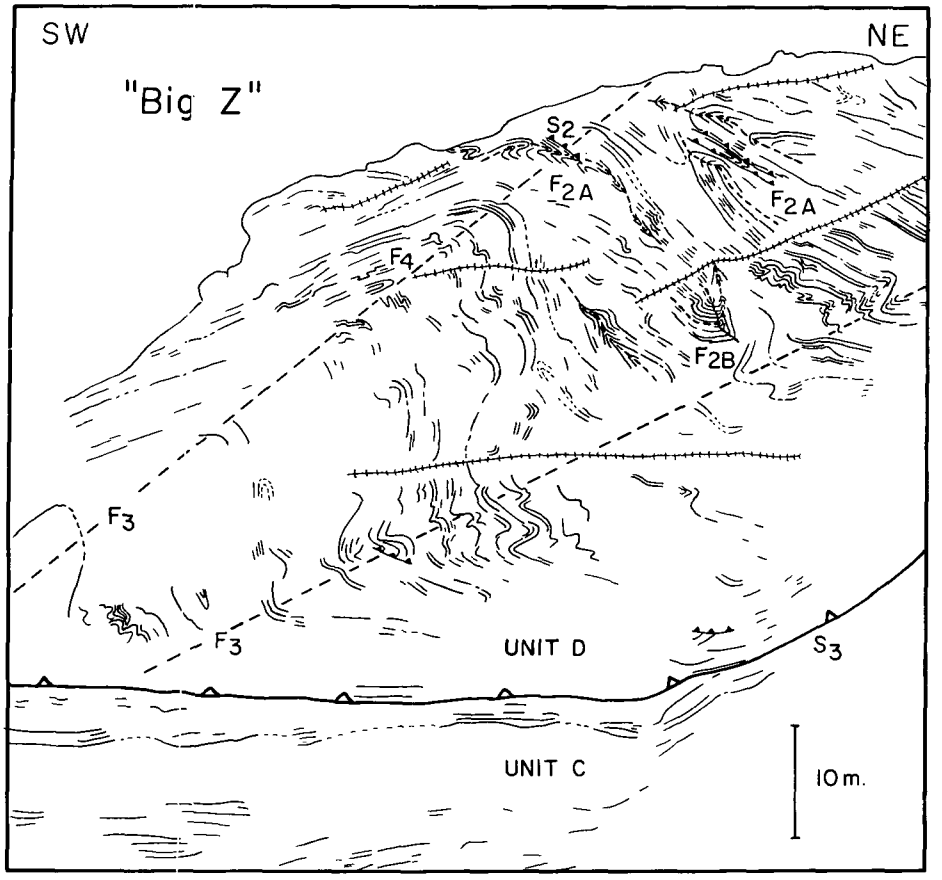

Figure 9. "Big Z" in unit D, Hoffman Canyon, Tobin Range. Oblique view of refolded folds. Shallow plunging, north-northwest-trending hinges of Big Z plunge down and to the right. Abundant tight to isoclinal, locally similar folds (labeled F_{2A}) are cut by faults (filled sawtooth pattern) and have axial surfaces folded around Big Z. One fold is refolded about another tight fold (labeled F_{2B}, right of center of sketch) that may also be pre-Big Z. Local box folds and folds of western vergence (labeled F_4) on the long limbs are post-Big Z (Mesozoic?). Chert layers can be traced across fracture zones (crosshatched lines). Large fault near bottom is Hoffman Canyon thrust. Structures traced from photo were shot from helicopter and measured in the field.

upper and lower contacts. Hinges (small dots) parallel solution-boudin lines (triangles) and plunge north to northeast, as opposed to the northwest-plunging folds in unit C-1 (Fig. 11A) and the partial northeast to northwest partial girdle distribution of hinges in unit C-3 (Fig. 11B). Axial surfaces (circles) dip steeply northwest, compared to the shallower dips of axial surfaces in units C-1 and C-3.

Fold hinges in units C-1 and C-3 are more scattered than are the relatively tightly clustered hinges in unit C-5. Composite packets usually display more variation in fabric orientations than do coherent packets like unit C-5, reflecting variations in orientations between any subunits that are separated by a thrust fault.

The observations described for units C-1, C-3, and C-5 apply to all packets in the Havallah sequence. Although most fold hinges of east-vergent folds plunge north, and most axial surfaces strike northeast and dip northwest, the orientations vary from packet to packet. The fact that these variations appear to occur across thrust-fault boundaries presumably reflects at least some rigid-body rotation during thrusting, but the fact that other fold properties, such as degree of appression, degree of overturning, fold profile, relationship to thrusts, and so forth, also vary from packet to packet suggests that different packets acquired different fabrics and potentially different fabric orientations and were juxtaposed by thrusting. Each packet thus has an individuality that distinguishes it from other packets. Variations in attitudes of hinges and axial surfaces from packet to packet are reflected in the large scatter on the summary diagrams (Figs. 10A and 10B) and further suggest that summary diagrams obscure important fabric details.

LOW-ANGLE FAULTS

Low-angle thrust faults are the dominant structural element of the Havallah sequence. The great number and the significance of these thrusts have not generally been recognized (except Turner, 1982) because they are usually parallel to subparallel to bedding and poorly exposed. Where exposures are good, we have been able to document numerous fault surfaces by the presence of discordant layering (Fig. 3), truncated folds, thin to thick (a few millimetres to several metres) cataclastic zones, surfaces with one, two, and even three generations of differently oriented slickensides, and subtle to radical changes in structural style and orientation between packets. The spacing between thrust surfaces varies from several centimetres to several metres. Younger low-angle thrusts cut older faults at several localities.

Some of these faults undoubtedly reflect displacements to resolve room problems created by disharmonic, flexural slip folding and, as such, are subordinate to folding. Most, however, have field relations that suggest far greater displacements than can be attributed to folding. Chert packets containing trains of harmonic folds occur next to unfolded chert packets (Fig. 3). Cherts with abundant solution boudins occur next to undistorted ribbon cherts. Some faults are occupied by clastic intrusions (see Fig. 13A below). The most obvious faults juxtapose packets of different lithology, internal structures, and, where fossil evidence is forthcoming, ages. For example, odd-numbered units C-1 through C-7 in Hoffman Canyon, Tobin Range (Fig. 2), are complexly folded and internally faulted chert-argillite packets of Pennsylvanian age, whereas the interleaved, even-numbered units C-2 through C-8 are relatively unfolded calcareous turbidites of Permian age (Stewart and others, 1977 and unpub. data). Few contacts between different rock types can be assumed to be depositional.

Cataclastic zones associated with faults range from extremely thin (a few millimetres) to several metres. Typically, they are composed of chert and argillite fragments enclosed in a much finer-grained matrix of chert, clay, and opaque material. The matrix tends to cleave along a

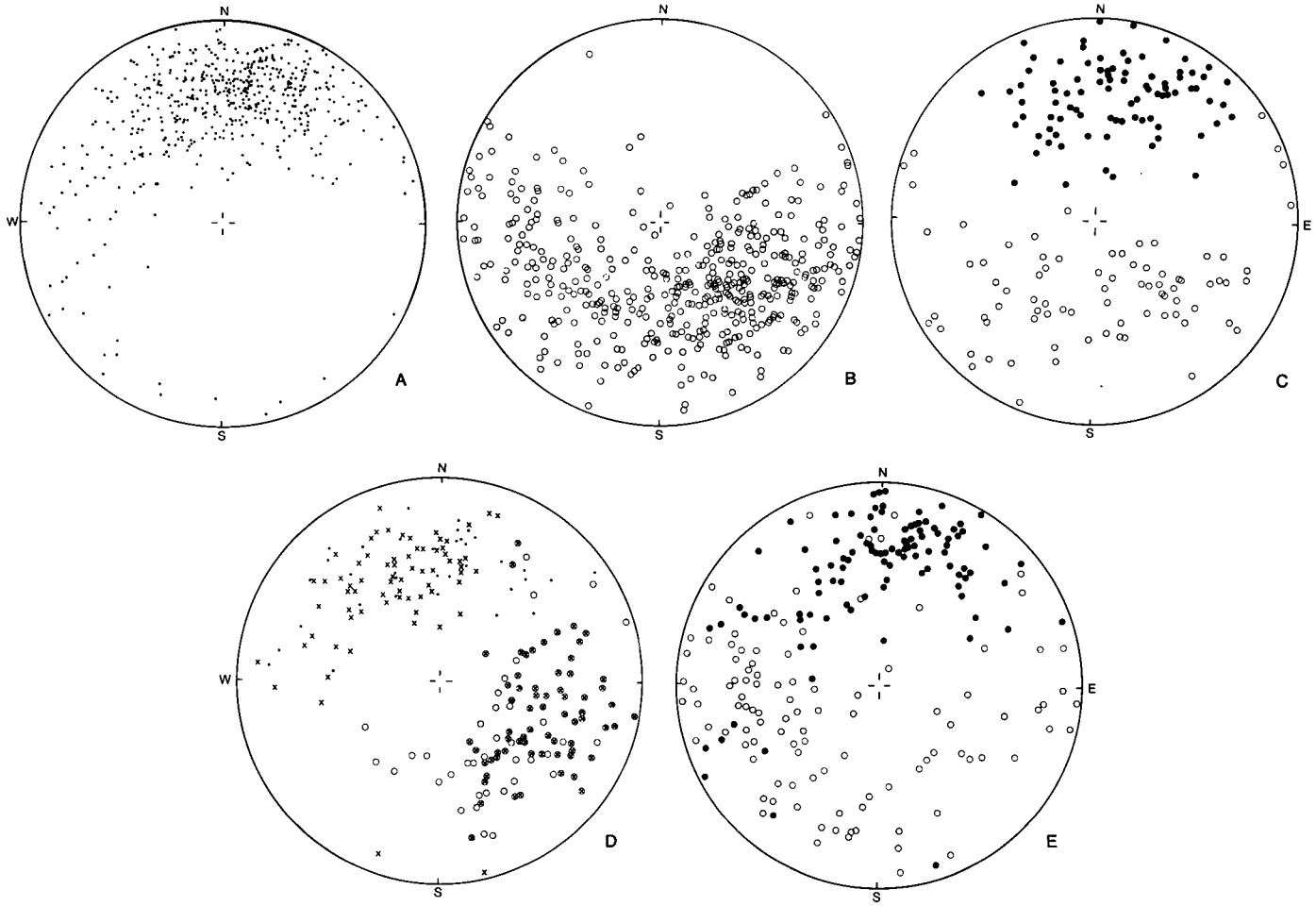

Figure 10. Equal-area plots of the fold fabric of the Havallah sequence in the Tobin Range. A. Hinges (dots) of all folds, regardless of generation, in the Tobin Range. Scattered hinges define a girdle with a strong maximum that plunges ~30° to the north; essentially the same fabric defined by lenticle lines (Fig. 7A). B. Poles to axial surfaces (empty circles) of all folds, regardless of generation, in the Tobin Range. Axial surfaces define a diffuse girdle perpendicular to maximum defined by hinges. C. Hinges (large dots) and poles to axial surfaces (empty circles) of all east-verging early folds, Tobin Range. D. Hinges (small dots and crosses) and poles (circles and circled crosses) to axial surfaces of late east-verging folds. Crosses represent structures measured near Big Z. E. Hinges (dots) and poles to axial surfaces (circles) of west-verging folds.

pronounced planar fabric which parallels the thrust-fault surface and which is defined by closely spaced (1 mm), subparallel films of clays and opaque material separating thin zones of fine-grained chert. The cleavage is locally folded and cut by small, low-angle, discrete displacement surfaces. Clasts vary in size from a few millimetres to several centimetres and may be either angular or rounded. Clasts with a distinct wispy or streaked-out appearance occur in some cataclastic zones from Frank Helen Canyon, Tobin Range (Turner, 1982). The cleavage conforms to the outlines of the clasts and is distorted where the clasts have been rotated. The cataclastic cleavage looks remarkably like the concentrated bedding-parallel microstylolites that occur in solution seams (see also Turner, 1982), except that it is more deformed, leading us to suspect that faults tended to exploit the clay-rich zones enhanced by bedding-parallel pressure solution and that slip was parallel to the microstylolites. Alternatively, the cleavage may be a fluxion texture created by simple shear parallel to the fault surface.

CHAOTIC ZONES

Closely spaced thrust surfaces and cataclastic zones create local composite thrust zones with interleafed coherent beds of folded or unfolded chert. A few exposures record thrusting that was distributed in zones that are tens of metres thick and enclose local isolated beds; rootless fold hinges; angular to rounded chert blocks; and milled-down, locally rotated chert phacoids. These fragments float in a matrix of sheared, fine-grained chert and argillite. Examples of thick chaotic zones are at Jim Creek, west Tobin Range (Fig. 2), and in drill cores from the Big Mike Mine and Frank Helen Canyon, east Tobin Range (Turner, 1982). Some of these zones contain exotic clasts (jasper, volcanic fragments) and may have originated as diamictites which resulted from sedimentary slumping. Others lack exotic clasts and contain rootless

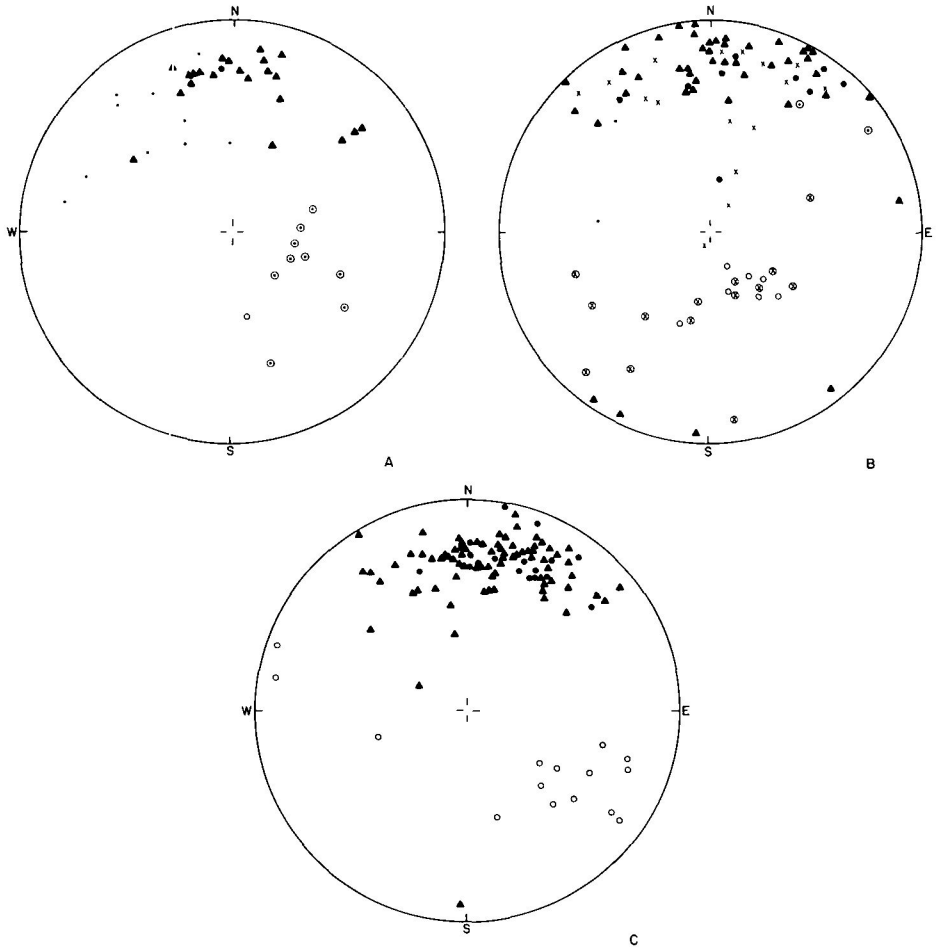

Figure 11. Fold and solution-boudin lines from three chert packets, units C-1 (11A), C-3 (11B), and C-5 (11C) of Stewart and others, 1977 (see Fig. 2), in Hoffman Canyon, Tobin Range, illustrating packet-to-packet variations in orientations. Hinges are large dots (early folds), small dots (late folds), or X's (either late or early). Axial surfaces are circles (early folds), circled dots (late folds), or circled X's (either late or early). Triangles are solution-boudin lines.

Figure 12. Dilation brecciation of chert from unit C-3, Hoffman Canyon, Tobin Range. Black and white chert layers were shattered into millimetre- to centimetre-sized, angular fragments which fit together (at A) where they had not been significantly rotated or translated. Green chert layers were pulverized to a much finer grain size (<1 mm), fluidized, and injected into the areas between the larger, separated fragments (clastic dike at B). Crack-seal fractures at C suggest an earlier episode of high pore-fluid pressure. Scale in centimetres.

folds that clearly predate shearing, suggesting that at least some of their chaotic character was the result of tectonism. Turner (1982) described an olistostrome in Frank Helen Canyon that displays a progressively stronger tectonic fabric as it is followed upsection toward the major thrust fault that separates lithotectonic units A and H (Fig. 2). Chaotic zones tend to be poorly exposed and may be more abundant than we have been able to document.

DILATION STRUCTURES

Crack-Seal Fractures

Veins filled mainly with quartz and/or chalcedony are locally abundant throughout the Havallah sequence (Figs. 4A and 4B). There may be several sets of these structures. Most are at high angles to bedding, are of variable strike, and tend to be restricted to one or a few chert layers. One set tends to occur in solution necks and parallels the trend of the boudin lines. Some veins are buckled and brecciated as a result of bedding-parallel dissolution. The vein-filling often shows a fibrous habit that is oriented perpendicular to the walls of the vein. Some contain one or more inclusion trains of wall-rock material near the center of the vein. Veins with similar antitaxial textures are called "crack-seal fractures" by Ramsay (1980) and appear to form by extension, with subsequent sealing by precipitation of crystalline material in the dilated zones.

Dilation Breccias

Coherent chert layers can be traced laterally to areas where the chert has been dismembered into angular fragments (Fig. 12). Fragments vary from a few millimetres to several centimetres and are separated by fine-grained, clay-rich siliceous material which intruded the spaces between chert fragments. Adjacent fragments clearly were together in coherent beds before brecciation, and there are no exotic fragments.

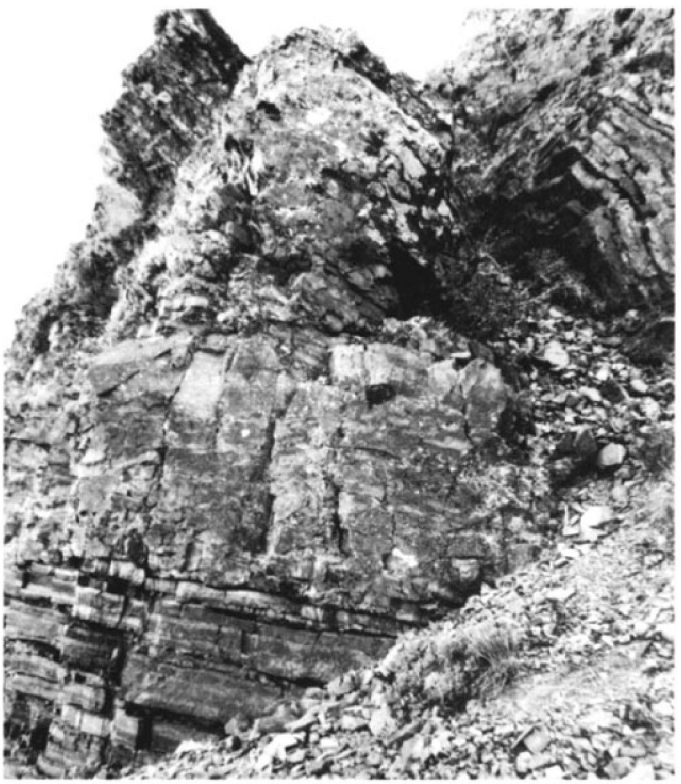

A

B

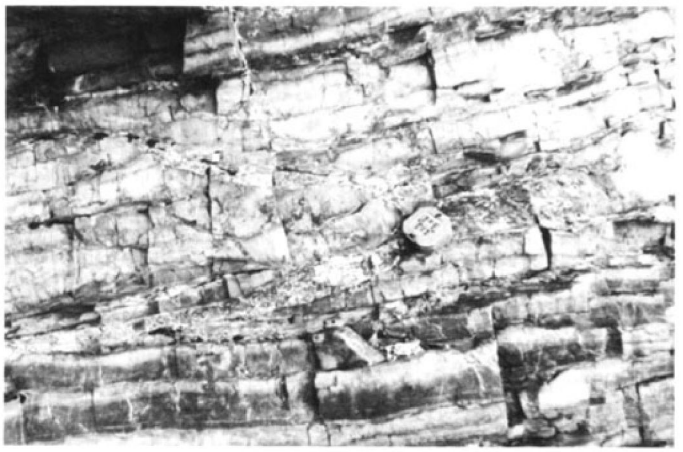

C

Figure 13. Clastic intrusions from unit K, station 31, Willow Creek, Battle Mountain (Fig. 3). A. Metre-thick "sill" occupying a thrust surface. Note discordant chert layering above and concordant layering within, and below, the sill. View is southwest. B. Along strike, the sill bifurcates and envelopes solution boudins in overlying packet. C. Thin clastic sill to right of brunton bifurcates into two crosscutting dikes to the left. Other thin sills are at top.

The fragments present an "exploded" appearance and can be fitted back together (Fig. 12). They are believed to be the result of distension or dilation, the fragments separating along preexisting planes of weakness (fractures, microstylolites, step planes, and so forth). Roehl (1981) described similar features in the Monterey Formation of California and called them "dilation breccias." We have documented only a few examples of dilation breccias in the Havallah sequence, but many of the breccias that we assumed formed by shear may have originated through the dilation mechanism.

Clastic Intrusions

Microscopic clastic dikes (1 or 2 mm in width; several centimetres in length) composed of fine-grained chert and clay were found, fortuitously, in several thin sections and polished slabs, suggesting that these features are common in the Havallah sequence. Megascopic dikes and injections concordant to bedding occur on the west side of Willow Creek, Battle Mountain (Figs. 13B and 13C); near the Big Mike Mine in west Tobin Range; and in Frank Helen Canyon, west Tobin Range (Turner, 1982). The intrusions at Willow Creek crosscut and laterally envelop both undeformed chert layers and solution boudins (Fig. 13B). The injected material is composed of rounded to angular fragments ranging in size from a few millimetres to several centimetres in a fine-grained matrix. The fragments include green and white chert and argillite (which could have been locally derived) and exotic material not found in nearby chert and argillite layers, including volcanic and plutonic clasts, single and composite quartz grains, and red jasperoid fragments. Some of the randomly oriented chert clasts contain a strong microstylolite fabric. The matrix contains a later set of microstylolites, and some clasts have been pressed together and dissolved along clast-clast contacts.

The clastic dikes merge downward and laterally into a tabular mass of variable thickness (3 cm to >1 m) that broadly parallels regional bedding. Chert layers above this body are discordant to the body, whereas the chert layers beneath the body are concordant (Fig. 13A), indicating that the mass occupies thrust surface. Clasts within the mass are slickensided and faceted, suggesting that the body has suffered cataclasis.

The presence of rounded clasts, clasts with a microstylolite fabric, and exotic fragments suggests that the material originated as sedimentary slump deposits or debris flows. It is not clear, however, whether the deposit was subsequently mobilized and injected as a clastic sill into a dilated, possibly active, thrust fault or whether it maintained its original depositional position, conformable upon the underlying chert, and subsequently was overridden by the overlying chert packet. Isolated fragments of chert layers within the main tabular mass are oriented paral-

lel to the boundaries of the body, as well as to the chert layers in the underlying packet (Fig. 13A). This suggests that the clastic material was injected in a "lit par lit" fashion (see also Fig. 13B). In either case, it is clear that the clastic material was fluidized and intruded as clastic dikes and sills into the overlying tectonic packet (Fig. 13C) during thrusting. A similar origin is suggested for the thinner tabular bodies that occur lower in the Willow Canyon section. Some of these sill-like bodies are, in turn, folded by east-verging parallel folds.

STRUCTURES IN OTHER ROCK TYPES

The fabrics described above are mainly from well-exposed chert. Associated argillites are less well exposed but appear to contain the same fabric as do the cherts. Most argillites display a moderate to strong cleavage which resembles the bedding-parallel microstylolite cleavage in chert. Folds are commonly isoclinal with similar profiles, indicating the the argillite behaved in a more ductile fashion than did most chert. Thick-bedded siliciclastic sandstones in Willow Canyon, Toquima Range, are deformed into large asymmetric buckle folds, but folds are rare in sandstones in other areas, perhaps because of their massive nature.

Permian calcareous turbidites that occur between chert packets in Hoffman Canyon, Tobin Range (Stewart and others, 1977 and unpub. data), are noteworthy in that they contain abundant slump folds but only a few east-vergent folds of clear tectonic origin. This fact was also noted by Stewart and others (1977 and unpub. data) and Turner (1982) in Frank Helen Canyon. The general lack of a pervasive fold fabric is puzzling in view of the abundant folds in neighboring Pennsylvanian chert packets. A possible reason for this lack of folds is developed below.

Breccias identified as slump deposits or debris flows contain fabrics of potential significance to the tectonic evolution of the Havallah sequence. The breccias are composed of angular to subrounded, clast-supported fragments in a finer-grained matrix of the same composition as are the clasts. Some examples contain exotic fragments (jasperoids, igneous rocks, and crystalline quartz) that could not have been derived from local lithologies. Others contain only chert, argillite, and siltstone fragments of presumed local derivation. Examples of locally derived slump deposits include a 5-m-thick unit in Frank Helen Canyon (Turner, 1982) and a folded, 10-m-thick unit that extends laterally for at least 50 m near the top of unit D in Lee Canyon, eastern Tobin Range.

The Lee Canyon exposure contains randomly oriented chert clasts with strong planar and linear fabrics expressed by microstylolites, microstylolite swarms, and micro-solution boudins (Fig. 14), fabrics that must have predated their deposition as slump deposits. The matrix contains a later generation of bedding-parallel microstylolites, indicating a bedding-normal loading event which postdated their deposition as slump deposits. This latter event caused some clasts to be pressed together and dissolved into each other (Fig. 14). Two fabric-forming events thus are separated by a cycle of erosion, slumping, and deposition.

SEDIMENTARY VERSUS TECTONIC FEATURES

Several of the features described from the Havallah sequence may have formed during deposition and early diagenesis prior to tectonism. These features should be distinguished from tectonic structures in order to unravel the structural evolution of the Havallah sequence, but this distinction is not always obvious. Brittle thrust faults and post-thrust structures are almost certainly tectonic in origin. These thrusts crosscut folds, high-angle fractures, quartz-chalcedony veins, and fabrics defined by bedding-parallel microstylolites, mound structures, step planes, and solution boudins. All of these early fabrics are potential diagenetic and/or sedimentary structures developed in an ocean-floor setting.

Keene (1975) described high-angle fractures, quartz-chalcedony veins, and breccias, which appear quite similar to the fractures, veins, and dilation breccias of the Havallah sequence, from DSDP Leg 32 cores of siliceous sediments in the northwestern Pacific Ocean. He ascribed their origin to volume changes during silica diagenesis. The random strikes of high-angle fractures and veins is consistent with formation in a nontectonic environment where lateral stresses are equal.

Mound structures, with their circular outlines (viewed normal to bedding), also probably formed while lateral stresses were equal. Concentric growth rings within mound structures indicate that their origin is related to the formation of chert nodules (Brueckner and others, unpub. data). Chert nodules are common in Deep Sea Drilling Project cores and are also found in the relatively undeformed Miocene Monterey Formation of California (Snyder and Brueckner, 1983). Mound structures in the Havallah sequence are generally outlined by microstylolite-rich solution seams. To our knowledge, similar microstylolite fabrics have not been described from siliceous sediments of modern ocean basins, but they do occur locally in the Monterey Formation (Snyder and Brueckner, 1983). The Monterey Formation is much thicker than most deep-sea siliceous sequences (Pisciotto, 1978), suggesting that bedding-parallel microstylolites can form only where the sediments are deeply buried. Possible mechanisms for achieving deep burial are presented below. We tentatively classify mound structures, associated microstylolites, some high-angle fractures and veins, and some dilation breccias as pretectonic structures (D_0) which formed during silica diagenesis while subjected to sedimentary loading.

We do not assign all bedding-parallel microstylolites to D_0, however. There are several phases of microstylolite development. Step planes, for example, offset an early microstylolite set and are, in turn, crosscut by later microstylolites (Fig. 4B). Some microstylolites postdate tectonic fractures. The clastic sill-like mass occupying a thrust fault in Willow Canyon contains microstylolites in the matrix and clasts that have been embayed into each other by pressure solution. Turner (1982) described folded microstylolites crosscut by later, unfolded microstylolites.

Solution boudins and step planes and associated microstylolites (henceforth called the "solution-boudin fabric") are tentatively re-

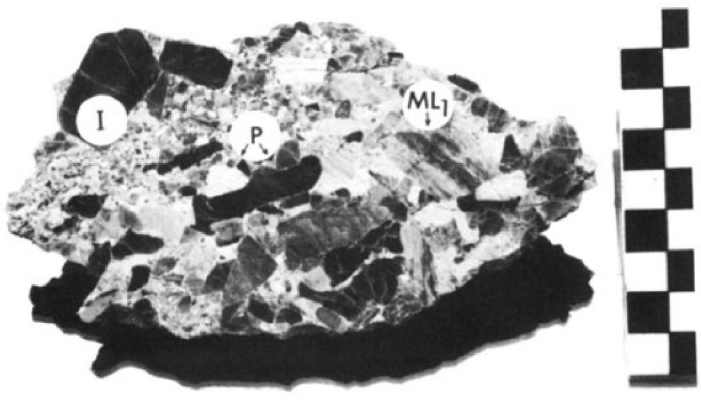

Figure 14. Polished slabs of slump breccia from unit D, Lee Canyon, Tobin Range. Clasts are believed to have been derived by erosion of previously tectonized chert. Several randomly oriented clasts contain tectonic fabrics composed of microstylolites and micro-solution boudins (ML_1). Fine-grained material appears to have injected (I) coarser fragments. Subsequent loading caused clasts to be pressed together and dissolved into each other (P). Scale in centimetres.

garded as early tectonic features (D_1) that formed while the sediments were still undergoing silica diagenesis (syntectonic diagenesis, Brueckner and others, unpub. data). Step planes and solution-boudin lines display a pronounced north-south–preferred orientation, suggesting east-west extension. Although it is possible that this extension could have been associated with downslope creep on east- or west-dipping paleoslopes, it is more likely that it occurred during tectonism. Solution boudins are outlined by microstylolite seams, and microstylolites both predate and postdate movement on step planes. These solution features require bedding-normal compression, which indicates that the sediments must have been deeply buried. Downslope creep and stretching presumably affects relatively shallow-level sediments.

Most pre-thrust folds deform the solution-boudin fabric (see below) and hence are also believed to be tectonic in origin; however, some isoclinal folds either predated or accompanied the formation of solution boudins and a strong microstylolite cleavage (Fig. 4A; see also Turner, 1982). These folds could be either tectonic or sedimentary structures. Slump features are scattered throughout the Havallah sequence (chert and multilithic breccias), and the Permian calcareous turbidites of Hoffman Canyon contain slump folds, convolute bedding, and other soft-sediment slope structures. There must have been paleoslopes present at some time during the evolution of the Havallah sequence, and the existence of slump folds in chert would not be surprising. The eastward vergence of these folds presents a problem, however, because the upper Paleozoic western margin of North America presumably dipped seaward (westward in present coordinates).

POLYPHASE DEFORMATION

If we are correct that the solution-boudin fabric is an early tectonic feature (D_1), then all structures that deform this fabric are also tectonic. All folds that deform a microstylolite cleavage are believed to be D_1 or later structures. Most fold hinges parallel solution-boudin lines, and many are not associated with step planes, rendering crosscutting relationships ambiguous. Where fold hinges do not parallel solution-boudin lines, however, the folds invariably fold the boudin lines. Similarly, where folds are associated with step planes, the step planes are either rotated about the fold hinge or have been reoriented to near parallelism with the fold axial surface by pressure solution. Folds that deform the microstylolite cleavage thus also deform the solution-boudin fabric wherever crosscutting relationships can be observed and can be assigned confidently to D_2 or younger fabrics. We suspect that this relationship is true for all post-microstylolite cleavage folds. We suggest that the parallelism of fold hinges and solution-boudin lines is at least partly the result of the linear anisotropy created in chert layers by solution-boudin lines. This anisotropy (thin solution necks, step planes) may have constrained the orientation of subsequent fold hinges and would explain the fact that the hinges of numerous folds are occupied by solution necks.

F_2 folds are further subdivided by their relationship with thrust faults. Folds that are offset by thrust faults are classified as F_{2A} folds; folds that deform thrust faults are classified as F_{2B}. F_{2A} folds tend to be tight, harmonic structures which deform entire chert packets. Many contain layers that deformed in a ductile fashion (class 1C or 2). Refolded F_{2A} folds have been observed by us and others (Miller and others, 1982, 1984; Macmillan, 1972 and unpub. data; Turner, 1982) at several localities. Unfortunately, we have not been able to document the relationship between the second-phase folds and thrust faults.

F_{2B} folds tend to be disharmonic open folds that deform only portions of chert packets. Clearly, most formed by flexural slip. They deform not only the thrust fault but also the chert packets on either side.

Where relationships between thrust faults and F_2 folds cannot be determined, there is a temptation to divide folds into F_{2A} or F_{2B} on the basis of their geometries. The second-phase folds that refold F_{2A} folds are generally disharmonic and open and have scattered distributions; we suspect that they are F_{2B} folds. There are enough exceptions to the generalizations presented above, however, to make this assignment uncertain.

The hinges of F_{2A} folds are locally associated with solution cleavage subparallel to the fold axial surface. Spaced (0.5 to 3 cm) stylolitic solution cleavage at high angles to bedding occurs in some unfolded chert layers. These surfaces crosscut microstylolites associated with solution boudins and hence are D_2 or later structures. All examined F_{2B} folds lack an axial-surface solution cleavage, but the rotated step planes appear to have suffered pressure solution.

We provisionally assigned some dilation structures to D_0; however, others deform or crosscut the solution-boudin fabric, and we attribute these structures to high fluid pressure during tectonism. There are quartz and chalcedony veins (crack-seal fractures), some of which contain two or more phases of vein material which are not brecciated and/or buckled in microstylolite-rich zones, suggesting that they formed after the microstylolites. The dilation breccia shown in Figure 12 disrupts chert horizons consisting of solution boudins and hence is clearly post-D_1. The best evidence is the association of clastic intrusions with a thrust fault in Willow Creek, Battle Mountain (Fig. 13). There, the clastic material also envelopes and intrudes solution boudins, and one clastic sill is folded by an F_{2B} fold. These crosscutting relationships document an episode of high pore-fluid pressure which postdated D_1, accompanied thrusting (D_2), and predated the development of F_{2B} folds.

Episodes of high pore fluid may have alternated with episodes of low pore-fluid pressure and pressure solution associated with bedding-normal loading. The clastic intrusions from Willow Canyon contain bedding-parallel microstylolites and clasts that have been dissolved into one another.

Mapping by Laule and others (unpub. data) in the Toquima Range indicates that the Golconda thrust crosscuts the internal thrusts that divide the Havallah sequence into tectonic packets. A similar relationship occurs at Willow Creek, Battle Mountain (Snyder, unpub. data). The Golconda thrust (and possibly other major thrusts), as well as associated folds, therefore postdate thrusting associated with D_2. Minor folds occur within 20 m of the Golconda thrust in the underlying autochthonous rocks in the New Pass Range (Macmillan, 1972 and unpub. data). Very large east-verging folds occur above the Golconda thrust in the Toquima Range (Laule and others, unpub. data) and above the Hoffman Canyon thrust in the Tobin Range (Big Z, Fig. 9). These larger folds deform several chert packets and one (probably two) previous fold phase. These structures, which mark the obduction of the Golconda allochthon onto North America, are assigned to a separate deformational event, D_3. Some, or possibly all, of the folds that we have designated F_{2B} may actually be F_3 folds.

A few small-scale, west-verging, open, buckle folds deform both limbs and the axial surface of F_2 folds. Other west-verging folds deform the cataclastic fabric of the Golconda thrust in Edna Mountain near Golconda Summit and in Willow Canyon in the eastern Toquima Range (Laule and others, unpub. data). These folds mark the last small-scale folding episode to affect the Havallah sequence (D_4) in the areas which we have studied. West-verging folds of similar orientation occur in the Triassic Auld Lang Syne Group, immediately north of Winnemucca, and in Clearwater Canyon, Sonoma Range, where they are associated with west-directed thrust faults (Gilluly, 1967; Silberling, 1975). F_4 folds thus may be Mesozoic structures that postdate the Sonoma orogeny. West-verging folds that occur on the short limbs of east-verging folds, or occur together with east-verging folds to form box folds, are not assigned to this event.

STRUCTURAL CHRONOLOGY

The Havallah structural fabric is clearly polyphase. We have not found a single chert packet that contains all, or even most, of the fabrics

found in the Havallah sequence. Were such a packet to exist, we believe it would have recorded structures in the order presented in Table 1. The list was compiled by determining the relative order of events in packets that contain two or more crosscutting fabrics and correlating the sequence of events in different packets by comparing common structural elements. With few exceptions, the sequence of events was the same in all packets.

A distinction must be made between structures that predate and those that postdate the D_2 thrusts that separate tectonic packets. Pre-D_2 thrust structures (D_0, D_1, D_{2A}, henceforth called internal structures) in one packet did *not* necessarily form at the same absolute time as did identical structures in other packets. This point deserves emphasis: D_2 thrust faults juxtapose packets that appear to have undergone the same order of structural events, but the structures recorded in one packet could have formed at totally different times than did structures in adjacent packets. The only constraints as to when internal deformation occurred in any given packet is that it postdated deposition and predated or accompanied thrusting. A further important consideration is that D_2 thrusting did not necessarily occur at one time; different packets could have been thrust together at totally different times. The only structures that can be assumed to have formed more or less synchronously are structures that developed after the entire Havallah sequence had been assembled (D_4 and, perhaps, D_3).

TABLE 1. STRUCTURAL EVENTS OF THE HAVALLAH SEQUENCE, NORTH-CENTRAL NEVADA

Event	*Fabric elements*	*Orientation*	*Comments*
D_0	Fractures and qtz-veins, microstylolites (C_0), mound structures, dilation breccias? Slumps?	Fractures and veins variable, at high angles to beds. C_0 parallels bedding.	Sedimentary loading. Fractures and veins from volume changes during diagenesis.
D_1	Solution boudins, step planes, further formation of microstylolites (C_1), isoclinal folds with C_1 axial cleavage?	C_1 parallel to bedding. Step planes strike north-south. Boudins form north-plunging maximum.	Early tectonics with bedding-normal loading; some east-west extension. Extreme thinning by solution.
	Thrusting, cataclastis, tight to open folds, east-verging folds (F_2), solution cleavage (C_2), breccias and fractures by high pore pressure.	Folds parallel boudin line. C_2 at high angles to bedding. Thrusts at very low angles to bedding.	East-directed thrusting in accretionary prism. Chert packets juxtaposed. Episodes of high and low pore pressures.
	Asymmetric folds (F_{2A}) predate thrusts or refolded. C_2 in hinges.	Generally north-plunging hinges. Axial surfaces refolded.	Folds usually tight or chevron, local ductile behavior.
	Thrusts, thrust zones, clastic intrusions.	Very low angles to bedding.	Several generations of thrusts.
D_2	Asymmetric folds (F_{2B}), concentric, post-thrust.	Generally north-plunging hinges.	Folding more disharmonic than F_{2A}.
D_3	Golconda thrust and major internal thrusts. Large asymmetric concentric folds (F_3), vergence east.	Folds parallel D_2 fold fabric. Major thrusts cut off D_2 thrusts.	Permian-Triassic obduction onto North American craton (Sonoma orogeny).
D_4	Asymmetric, gentle to open concentric folds (F_4), vergence west.	Scattered, generally north-plunging.	Possibly related to Mesozoic events.

BACK-ARC THRUSTING VERSUS FAR-TRAVELED ACCRETIONARY PRISM

The accretionary prism interpretation remains the most viable for explaining the structural evolution of the Havallah sequence (Speed, 1979). Pillow basalts and other greenstones, generally believed to represent the ocean-crust basement to the sediments, occur only locally in the sequence, generally at the base of thrust slices. The rest of the oceanic crust must have been detached and removed, presumably by underthrusting into the mantle. The eastward vergence of F_1 through F_3 folds is consistent with westward underthrusting of oceanic crust. The numerous thrust faults, chaotic zones, asymmetric folds, and structures suggesting episodes of high pore-fluid pressures are features that characterize accretionary prisms.

Both the back-arc basin and the far-traveled arc models discussed in the introduction can accommodate an accretionary prism interpretation for the Havallah sequence. The differences between the models are those of scale. The far-traveled arc model requires the subduction of thousands of kilometres of oceanic crust. Protracted geologic time would be required to subduct so much material, and the sediments that initially overlay the oceanic crust would have had to undergo an enormous amount of structural telescoping if they were stacked as imbricate thrusts in the prism. In contrast, closing a relatively narrow (tens to a few hundred kilometres) marginal basin requires relatively limited underthrusting of oceanic basement (not enough to generate a volcanic arc). This process could occur within a relatively short time span and with relatively limited structural stacking of the offscraped sediments.

The parts of the Havallah sequence which we have studied contain very large numbers of fault-bounded tectonic packets. If these observations hold true for the entire allochthon, then the amount of shortening implied by these structures is vastly greater than previously realized. The shortening suggested by the six or more major lithotectonic units that occur in most ranges (Fig. 2) is already considerable. The exact thicknesses and number of packets contained in each lithotectonic unit are difficult to determine, but there are at least 6 tectonic packets in the basal 200 m of lithotectonic unit 3, Battle Mountain (Fig. 3). Even a very conservative approach, based strictly on fossil evidence for structural repetitions, indicates a minimum of 8 tectonic packets in the nearly 1,800-m-thick exposure of unit C, Hoffman Canyon (Stewart and others, unpub. data).

Precise estimates of the amount of structural shortening of the Havallah sequence cannot be made because displacements along the faults are unknown. Even if these displacements were known, they would provide only minimum estimates for the amount of underthrust oceanic basement, as it cannot be assumed that all of the sediments deposited in the Havallah basin were accreted into the prism. Nevertheless, the very large number of faults makes it more likely that the Havallah sequence was severely telescoped and that a large amount of oceanic crust was subducted. The discovery of these faults increases the plausibility of the far-traveled accretionary prism model.

The Havallah structural fabric is polyphase, much more so than is generally recognized (however, see Babaie and Speed, 1983; and J. R. Macmillan, unpub. data). We have been very conservative about assigning structures to separate deformational events (Table 1). For example, the D_2 fabric is, itself, clearly polyphase. There are at least three east-verging folding phases (F_{2A}, F_{2B}, F_3; there are four such phases if F_1 folds are tectonic) and two thrusting episodes (associated with D_2 and D_3, respectively) interspersed or associated with periods of high pore-fluid pressure (dilation structures) and periods of bedding-normal loading (bedding-parallel microstylolites and solution boudins). The absence of absolute dating of structural events makes it impossible to determine with certainty whether these events occurred within a relatively short period of time or extended over a protracted time interval. Nevertheless, we favor the latter for the following reasons.

1. Different packets probably received their internal structures at different times. Under otherwise identical conditions (stress, temperature, pressure, and so forth), different structures will result, depending on whether the sediments were deformed while unlithified, weakly lithified, or completely lithified. The relationship between the lithic state of sediments and the timing of deformation is of particular interest when applied to siliceous sediments (Siever, 1983). The silica in these sediments undergoes a series of diagenetic polymorphic conversions during burial which converts the amorphous opal-A (terminology of Jones and Segnit, 1971) of siliceous organisms successively to, first, a disordered

mixture of cristobalite and tridymite (opal-CT) and then to highly ordered diagenetic quartz. The structural responses to stress of siliceous sediments in different diagenetic states are explored in detail in other papers for the Monterey Formation of California (Snyder and others, 1983) and the Havallah sequence (Brueckner and others, unpub. data). The solubility of silica in aqueous solutions decreases sharply with increasing diagenesis (Kastner, 1979). Furthermore, the siliceous sediments associated with each diagenetic state have markedly different rheologies as a result of changes in porosity, permeability, rigidity of the silica polymorphs, and so forth. We suggest, to a first approximation, and all other variables (strain rate, pore-fluid pressure, and so forth) being equal, that diagenetically immature siliceous sediments that consist of opal-A should be more soluble and ductile than are diagenetically mature quartzose rocks. Moreover, the conversions of opal-A to opal-CT to quartz are also dehydration reactions, because opal-A can contain as much as 20 wt % water (Kastner, 1979). The release of this structurally bonded water during diagenesis should result in episodes of high pore-fluid pressures.

Some of the oldest chert packets (Late Devonian–Early Mississippian) of the Havallah have the same structures and sequence of structural events as do the youngest chert packets (early Late Permian). Among these structures are early folds that deformed largely, or in part, by ductile flow. Similarly, solution features such as bedding-parallel and bedding-normal microstylolites, solution boudins, and so forth, appear to be developed to the same degree in Mississippian cherts as in Permian cherts. If our silica diagenesis-deformation model is correct, these solution features and ductile folds indicate that deformation occurred before some of the oldest siliceous sediments had undergone significant silica diagenesis to relatively rigid, insoluble quartz chert. This reasoning implies that these siliceous sediments were deformed within a few *tens of millions of years after deposition.* If deformation were restricted entirely to the classical Permian-Triassic Sonoma orogeny, the older siliceous sediments should have completed diagenesis, as a result of burial by Upper Mississippian, Pennsylvanian, and Permian clastic and siliceous sediments, within the long interval (~120 m.y.) of time between deposition and tectonism. The short-lived, back-arc thrusting model should result, therefore, in relatively brittle deformation for old chert packets. Ductile deformation should be restricted to the thin veneer of young, diagenetically immature siliceous sediments.

The uncertainty to this argument lies in the initial (depositional) thickness of the Havallah sequence. Thin siliceous sequences can remain in lower diagenetic states much longer than can thick sequences (Pisciotto, 1981), and the arguments presented above may be less valid if the Havallah sequence was too thin to complete silica diagenetic transformations in its basal portions prior to deformation. Unfortunately, the initial thickness of the Havallah sequence may never be determined with certainty, even if all structural repetitions by thrusting are removed, because of two processes with opposite effects: (1) bedding-parallel pressure solution has thinned the Havallah sequence; (2) folding has thickened it.

2. Unfolded Permian calcareous turbidites suggest pre-Permian deformation. We refer specifically to almost undeformed Permian calcareous turbidites (units C-2 through C-8) in Hoffman Canyon (Fig. 2) which lie above Pennsylvanian cherts (units C-1 through C-7) with complex, locally polyphase folds and other internal fabrics. We suggest that the older cherts were deformed prior to the Permian deposition of the turbidites and that the contact between the two is an unconformity. The contacts are not well enough exposed, however, to determine whether they are tectonic rather than depositional. An alternate explanation, that the calcareous turbidites were too rigid to fold along with the cherts, is considered less likely because most of the beds are thinly laminated, many contain a high amount of relatively ductile carbonate, and they contain some local late folds near thrust contacts which we assign to D_{2B} or D_3.

3. Slump deposits contain clasts with predepositional structural fabrics. Chert fragments within the slump breccia near the top of unit D in Lee Canyon contain bedding-parallel microstylolites and micro-solution boudins (Fig. 14). The age of these clasts is unknown. They could have been derived from lower Paleozoic cherts of the Antler orogenic belt. If, however, the clasts were from upper Paleozoic cherts, they would indicate two episodes of tectonism separated by an interval of exposure, erosion, and deposition, ("recycled" sediments) and demonstrate prolonged deformation.

Each of the preceding arguments contains ambiguities; however, if combined with the polyphase nature of the Havallah fabric, they strongly indicate to us that deformation was protracted and resulted in a tremendous amount of shortening. For these reasons, in addition to a series of arguments presented elsewhere (Snyder and Brueckner, 1983), we favor the far-traveled accretionary prism model to explain the structural evolution of the Havallah sequence.

CONCLUSIONS

The dynamics of far-traveled accretionary wedges can explain why chert of widely different ages underwent similar strain histories at different times. Barring radical shifts in the relative motion between the underthrusting and overriding plate, the toe of an accretionary prism can present a stable strain environment (that is, relatively constant orientations and magnitudes of the principal strain axes) for as long as subduction continues. It therefore is expected that sediments accreted during the early history of an accretionary wedge should broadly exhibit the same structural fabric, orientations, and sequence as sediments that were added later. Folds that formed at different times, for example, could be expected to be coaxial.

The accretionary prism model does, however, provide for subtle shifts in the strain environment. Convergence rates between tectonic plates can change, thereby changing strain rates within the prism (Moore, 1979). Furthermore, older packets and their internal structures will be rotated up and toward steeper orientations as new material is accreted beneath the toe of the prism. This feature can, for example, cause faults to be rotated out of positions of optimum shear, resulting in the formation of new faults at low angles to the old faults or in the development of other structures, such as folds. These shifts are a likely explanation for the polyphase structural fabric of the Havallah sequence.

We therefore model the deformational sequence that produced the Havallah fabric as follows. D_0, diagenesis of siliceous sediments on the sea floor resulted in the formation of fractures, veins, mound structures, and the initial development of bedding-parallel microstylolites.

D_1 (Early Accretion)

Sedimentary and/or tectonic loading, combined with either the arching of the ocean crust as it neared the subduction zone or extension within the toe of the accretionary prism (as suggested by seismic first-motion studies, Wang, 1980), caused siliceous sediments to be slightly stretched in an east-west direction, setting the orientations of north-south–trending step planes. Synchronous or subsequent bedding-parallel solution modified the rhomboid chert blocks between step planes to form solution boudins. Loading could have been caused by two processes. As the sediments neared the accretionary prism, turbidites, debris flows, and clastic sediments were deposited on the siliceous sediments, enhancing the sedimentary load. Further tectonic loading occurred as siliceous sediments were tucked beneath the accretionary prism. Sedimentary and/or tectonic loading caused accelerated development of the microstylolite cleavage. There was probably some F_1 folding during initial accretion, but we have found only two folds with an axial-surface microstylolite cleavage.

D_2 (Main Phase Accretion)

As successive packets of siliceous sediments were underthrust westward beneath the toe of

the prism, siliceous sediments deformed heterogeneously, according to the rheology and solubility set by their diagenetic state (Brueckner and others, unpub. data). Diagenetically immature siliceous sediments could have acted as ductile strain accumulators, allowing the more rigid, diagenetically mature sediments to escape deformation and retarding the development of tectonic mélanges. Diagenetic transformation rates were accelerated as a result of tectonic thickening, resulting in the progressive embrittlement of the siliceous sediments. The crystallographically bound water released by these reactions, combined with reductions in permeability and porosity by recrystallization and compaction, helped to create high pore-fluid pressure and encouraged thrusting, brecciation, and the injection of clastic intrusions. High pore-fluid pressures and the existence of diagenetically mature, rigid chert packets encouraged shear to occur along discrete thrust surfaces rather than disrupting thick zones to form tectonic mélanges. High pore-fluid pressures may have caused aseismic thrusting, a characteristic of accretionary prisms (Wang, 1980). These processes occurred continuously during much of the upper Paleozoic as new sediments, including recycled slump deposits, were tucked in beneath the prism. Each introduced packet may have acquired its internal structural fabric during a single progressive deformation; however, different packets were deformed at different times as they were introduced into the prism. As the prograding prism and island arc neared North America in Permian time, calcareous turbidites, derived from shelf carbonates either from North America or the arc, were deposited on top of the accretionary prism and subsequently shuffled into the top of the prism by reactivation of faults.

D_3 (Obduction)

Ultimately, the Havallah basin closed via subduction, and the accretionary prism was thrust over North America along the Golconda thrust in the Permian-Triassic. Some of the major thrusts and large asymmetric folds within the Havallah sequence formed during obduction. If our model is correct, the Sonoma "orogeny" should be considered a tectonic cycle that closed a major ocean basin and spanned the middle Paleozoic to the Permian-Triassic rather than a short, discrete compressional event in Permian-Triassic time.

ACKNOWLEDGMENTS

We thank Ian Dalziel, Steve Marshak, Jim Helwig, D. K. Larue, Bob Turner, Elizabeth Miller, Greg Davis, and an anonymous reviewer for critically reviewing earlier versions of this manuscript; Mary Ann Luckman for her technical help; and Steve Goldstein and Bill Devlin for their able field assistance. Elizabeth Miller, Bob Speed, Susan Laule, and many others tried to keep us honest about interpreting the Havallah structural fabric. Carolyn Isaacs, Ken Pisciotto, James Hein, and Charlotte Schreiber have been very helpful to us in our attempts to understand silica diagenesis. The work was supported by National Science Foundation Grants EAR-78-23585, EAR-79-05722, and EAR-79-11301.

REFERENCES CITED

Alvarez, W., Engelder, T., and Lowrie, W., 1976, Formation of spaced cleavage and folds in brittle limestone by dissolution: Geology, v. 4, p. 698–701.

Babaie, H. A., and Speed, R. C., 1983, Significance of tectonic fabric of the Golconda allochthon in Toiyabe Range, Nevada: Geological Society of America Abstracts with Programs, v. 15, p. 382.

Burchfiel, B. C., and Davis, G. A., 1975, Nature and controls of Cordilleran orogenesis, western United States: Extensions of an earlier synthesis: American Journal of Science, v. 272, p. 97–118.

Dickinson, W. R., 1977, Paleozoic plate tectonics and the evolution of the Cordilleran continental margin, *in* Stewart, J. H., Stevens, C. H., and Fritsche, A. E., eds., Paleozoic paleogeography of the western United States: Society of Economic Paleontologists and Mineralogists, Pacific Coast Paleogeography Symposium 1, p. 137–156.

Erickson, R. L., and Marsh, S. P., 1974, Geologic map of the Golconda quadrangle, Humboldt County, Nevada: U.S. Geological Survey Geologic *Quadrangle Map, GQ-1174, scale 1:24,000.*

Ferguson, H. G., Muller, S. W., and Roberts, R. J., 1951a, Geology of the Winnemucca quadrangle, Nevada: U.S. Geological Survey Geologic Quadrangle Map GQ-11, scale 1:125,000.

——1951b, Geology of the Mount Moses quadrangle, Nevada: U.S. Geological Survey Geologic Quadrangle Map GQ-12, scale 1:125,000.

Ferguson, H. G., Roberts, R. J., and Muller, S. W., 1952, Geology of the Golconda quadrangle, Nevada: U.S. Geological Survey Geologic Quadrangle Map GQ-15, scale 1:125,000.

Gilluly, J., 1967, Geologic map of the Winnemucca quadrangle, Pershing and Humboldt Counties, Nevada: U.S. Geological Survey Geologic Quadrangle Map GQ-656, scale 1:62,500.

Jenkyns, H. C., and Winterer, E. L., 1982, Palaeoceanography of Mesozoic ribbon radiolarites: Earth and Planetary Science Letters, v. 60, p. 351–375.

Jones, J. B., and Segnit, E. R., 1971, The nature of opal. I. Nomenclature and origin of constituent phases: Geological Society of Australia Journal, v. 18, p. 57–68.

Kastner, M., 1979, Silica polymorphs, *in* Burns, R. G., ed., Mineralogical Society of America Short Course Notes: Marine Minerals, v. 6, p. 99–107.

Keene, J. B., 1975, Cherts and porcelanites from the North Pacific, DSDP Leg 32, *in* Larson, R. L., Moberly, R., and others, eds., 1975, Initial reports of the Deep Sea Drilling Project, Volume 32: Washington, D.C., U.S. Government Printing Office, p. 429–447.

Laule, S. W., Snyder, W. S., and Ormiston, A. R., 1981, Willow Canyon Formation: An extension of the Golconda allochthon: Geological Society of America Cordilleran Section meeting, San Jose, California, 1981, Abstracts with Programs, p. 66.

Macmillan, J. R., 1972, Late Paleozoic and Mesozoic tectonic events in west-central Nevada [Ph.D. dissert.]: Evanston, Illinois, Northwestern University, 146 p.

Miller, E. L., Bateson, J., Dinter, D., Dyer, J. R., Harbaugh, D., and Jones, D. L., 1981, Thrust emplacement of the Schoonover sequence, northern Independence Mountains, Nevada: Geological Society of America Bulletin, v. 92, p. 720–737.

Miller, E. L., Kanter, L. R., Larue, D. K., Turner, R. J., Murchey, B., and Jones, D. L., 1982, Structural fabric of the Paleozoic Golconda allochthon, Antler Peak quadrangle, Nevada: Progressive deformation of an oceanic sedimentary assemblage: Journal of Geophysical Research, Special Issue on Accretionary Tectonics, v. 87, p. 3795–3804.

Miller, E. L., Holdsworth, B. K., Whiteford, W. B., and Rodgers, D., 1984, Stratigraphy and structure of the Schoonover sequence, northeastern Nevada: Implications for Paleozoic plate-margin tectonics: Geological Society of America Bulletin, v. 95, p. 1063–1076.

Moore, J. C., 1979, Variation in strain and strain rate during underthrusting of trench deposits: Geology, v. 7, p. 185–188.

Muller, S. W., Ferguson, H. G., and Roberts, R. J., 1951, Geology of the Mount Tobin quadrangle, Nevada: U.S. Geological Survey Geologic Quadrangle Map GQ-7, scale 1:125,000.

Nelson, K. D., 1982, A suggestion for the origin of mesoscopic fabric in accretionary melange, based on features observed in the Crystalls Beach Complex, South Island, New Zealand: Geological Society of America Bulletin, v. 93, p. 625–634.

Pisciotto, K. A., 1978, Basinal sedimentary facies and diagenetic aspects of the Monterey Shale, California [Ph.D. thesis]: Santa Cruz, California, University of California, 450 p.

——1981, Distribution, thermal histories, isotopic compositions and reflection characteristics of siliceous rocks recovered by the Deep Sea Drilling Project, *in* Warme, J. E., Douglas, R. G., and Winterer, E. L., eds., The Deep Sea Drilling Project: A decade of progress: Society of Economic Paleontologists and Mineralogists Special Publication 32, p. 129–148.

Ramsay, J. G., 1967, Folding and fracturing of rocks: New York, McGraw-Hill, 568 p.

——1980, The crack-seal mechanism of rock deformation: Nature, v. 284, p. 135–139.

Roberts, R. J., 1951, Geology of the Antler Peak quadrangle, Nevada: U.S. Geological Survey Geologic Quadrangle Map GQ-10, scale 1:62,500.

——1964, Stratigraphy and structure of the Antler Peak quadrangle, Humboldt and Lander Counties, Nevada: U.S. Geological Survey Professional Paper 459A, 93 p.

Roehl, P. O., 1981, Dilation brecciation—A proposed mechanism of fracturing, petroleum expulsion and dolomitization in the Monterey Formation, California, *in* Garrison, R. E., Douglas, R. G., and others, eds., The Monterey Formation and related siliceous rocks of California: Society of Economic Paleontologists and Mineralogists, Pacific Section, p. 285–316.

Rye, R. O., Roberts, R. J., Snyder, W. S., Lahusen, L. H., and Mottica, J. E., 1984, Textural and sulfur isotopic studies of Big Mike cupriferous volcanogenic massive sulfide deposit, Pershing County, Nevada: Economic Geology, v. 79, p. 124–140.

Schweickert, R. A., and Snyder, W. S., 1981, Paleozoic plate tectonics of the Sierra Nevada and adjacent regions, *in* Ernst, W. G., ed., The geotectonic evolution of California: Englewood Cliffs, New Jersey, Prentice-Hall, Inc., p. 182–202.

Siever, R., 1983, Evolution of chert at active and passive continental margins, *in* Iijima, A., and others, eds., Siliceous deposits of the Pacific region: Developments in Sedimentology, v. 36, p. 7–24.

Silberling, N. J., 1973, Geologic events during Permian-Triassic time along the Pacific margin of the United States, *in* Logan, A., and Hills, L. V., eds., The Permian and Triassic systems and their mutual boundary: Calgary, Canada, Alberta Society of Petroleum Geology, p. 345–362.

——1975, Age relationships of the Golconda thrust fault, Sonoma Range, north-central Nevada: Geological Society of America Special Paper 163.

Silberling, N. J., and Roberts, R. J., 1962, Pre-Tertiary stratigraphy and structure of northwestern Nevada: Geological Society of America Special Paper 72, 58 p.

Snyder, W. S., 1977, Origin and exploration for ore deposits in upper Paleozoic chert-greenstone complexes of northern Nevada [Ph.D. thesis]: Stanford, California, Stanford University, 159 p.

——1978, Manganese deposited by submarine hot springs in chert-greenstone complexes, western United States: Geology, v. 6, p. 741–744.

Snyder, W. S., and Brueckner, H. K., 1983, Tectonic evolution of the Golconda allochthon, Nevada: Problems and perspectives, 1983, *in* Stevens, C. A., ed., Paleozoic and early Mesozoic rocks in microplates of western North America: Society of Economic Paleontologists and Mineralogists, Pacific Section, p. 103–123.

Snyder, W. S., Brueckner, H. K., and Schweickert, R. A., 1983, Deformational styles in the Monterey Formation and other siliceous sedimentary rocks, *in* Isaacs, C. M., and others, eds., Symposium volume on Monterey oil fields: Society of Economic Paleontologists and Mineralogists, Pacific Section, p. 103–123.

Snyder, W. S., Brueckner, H. K., and Schweickert, R. A., 1983, Deformational styles in the Monterey Formation and other siliceous sedimentary rocks, *in* Isaacs, C. M., and others, eds., Symposium volume on Monterey oil fields: Society of Economic Paleontologists and Mineralogists, Pacific Section, p. 151–170.

Speed, R. C., 1977, Island-arc and other paleogeographic terranes of late Paleozoic age in the western Great Basin, *in* Stewart, J. H., Stevens, C. H., and Fritsche, A. E., eds., Paleozoic paleogeography of the western United States: Society of Economic Paleontologists and Mineralogists, Pacific Coast Paleogeography Symposium 1, p. 349–363.

——1979, Collided Paleozoic platelet in the western United States: Journal of Geology, v. 87, p. 279–292.

Stewart, J. H., MacMillan, J. R., Nichols, K. M., and Stevens, C. H., 1977, Deep-water upper Paleozoic rocks in north-central Nevada—A study of the type area of the Havallah Formation, *in* Stewart, J. H., Stevens, C. H., and Fritsche, A. E., eds., Paleozoic paleogeography of the western United States: Society of Economic Paleontologists and Mineralogists, Pacific Coast Paleogeography Symposium 1, p. 337–347.

Taliaferro, N. L., 1934, Contraction phenomena in cherts: Geological Society of America Bulletin, v. 45, p. 189–232.

Turner, R.J.W., 1982, The geology of the east-central Tobin Range Nevada [Ph.D. dissert.]: Stanford, California, Stanford University, 113 p.

Wang, C. Y., 1980, Sediment subduction and frictional sliding in a subduction zone: Geology, v. 8, p. 530–533.

Wanless, H. R., 1979, Limestone response to stress: Pressure solution and dolomitization: Journal of Sedimentary Petrology, v. 49, p. 437–462.

Whiteford, W. B., Little, T. A., Miller, E. L., 1983, The nature of the Antler orogeny: View from north-central Nevada: Geological Society of America Abstracts with Programs, v. 15, p. 382.

MANUSCRIPT RECEIVED BY THE SOCIETY OCTOBER 29, 1984
REVISED MANUSCRIPT RECEIVED FEBRUARY 18, 1985
MANUSCRIPT ACCEPTED FEBRUARY 27,1985
LAMONT-DOHERTY GEOLOGICAL OBSERVATORY CONTRIBUTION NO. 3856

Printed in U.S.A.